

1 This paper is a non-peer reviewed preprint submitted to EarthArXiv, which has been submitted to a  
2 special publication of the American Geophysical Union for peer review.

3

4 **Seismic and Acoustic Monitoring of Submarine Landslides: Ongoing Challenges, Recent Successes**  
5 **and Future Opportunities**

6 Clare, M.A.<sup>1\*</sup>, Lintern, D.G.<sup>2</sup>, Pope, E.<sup>3</sup>, Baker, M.<sup>3</sup>, Ruffell, S.<sup>3</sup>, Zulkifli, Z.<sup>1</sup>, Simmons, S.<sup>4</sup>, Urlaub,  
7 M.<sup>5</sup>, Belal, M.<sup>1</sup>, Talling, P.J.<sup>3</sup>

8 1) National Oceanography Centre, Southampton, SO14 3ZH, UK

9 2) Natural Resources Canada, Geological Survey of Canada, Sidney, British Columbia V8L 4B2,  
10 Canada

11 3) Departments of Earth Sciences and Geography, University of Durham, Stockton Road, Durham,  
12 UK, DH1 3LE, UK

13 4) Earth and Environment Institute, Hull, UK

14 5) GEOMAR Helmholtz Centre for Ocean Research, Kiel, Germany.

15

16 \*Contact: [m.clare@noc.ac.uk](mailto:m.clare@noc.ac.uk)

17

18

19 **Seismic and Acoustic Monitoring of Submarine Landslides: Ongoing Challenges, Recent Successes**  
20 **and Future Opportunities**

21 Clare, M.A.<sup>1</sup>, Lintern, D.G.<sup>2</sup>, Pope, E.<sup>3</sup>, Baker, M.<sup>3</sup>, Ruffell, S.<sup>3</sup>, Zulkifli, Z.<sup>1</sup>, Simmons, S.<sup>4</sup>, Urlaub,  
22 M.<sup>5</sup>, Belal, M.<sup>1</sup>, Talling, P.J.<sup>3</sup>

23 6) National Oceanography Centre, Southampton, SO14 3ZH, UK

24 7) Natural Resources Canada, Geological Survey of Canada, Sidney, British Columbia V8L 4B2,  
25 Canada

26 8) Departments of Earth Sciences and Geography, University of Durham, Stockton Road, Durham,  
27 UK, DH1 3LE, UK

28 9) Earth and Environment Institute, Hull, UK

29 10) GEOMAR Helmholtz Centre for Ocean Research, Kiel, Germany.  
30

31 **Abstract**

32 Submarine landslides pose a hazard to coastal communities due to the tsunamis they can generate, and  
33 can damage critical seafloor infrastructure, such as the network of cables that underpin global data  
34 transfer and communications. These mass movements can be orders of magnitude larger than their  
35 onshore equivalents and are found on all of the world's continental margins; from coastal zones to hadal  
36 trenches. Despite their prevalence, and importance to society, offshore monitoring studies have been  
37 limited by the largely unpredictable occurrence of submarine landslide and the need to cover large  
38 regions of extensive continental margins. Recent subsea monitoring has provided new insights into the  
39 preconditioning and run-out of submarine landslides using active geophysical techniques, but these tools  
40 only measure a very small spatial footprint, and are power and memory intensive, thus limiting long  
41 duration monitoring campaigns. Most landslide events therefore remain entirely unrecorded. Here we first  
42 show how passive acoustic and seismologic techniques can record acoustic emissions and ground motions  
43 created by terrestrial landslides. We then show how this terrestrial-focused research has catalysed  
44 advances in the detection and characterisation of submarine landslides, using both onshore and offshore  
45 networks of broadband seismometers, hydrophones and geophones. We then discuss some of the new  
46 insights into submarine landslide preconditioning, timing, location, velocity and their down-slope  
47 evolution that is arising from these advances. We finally outline some of the outstanding challenges, in  
48 particular emphasising the need for calibration of seismic and acoustic signals generated by submarine

49 landslides and their run-out. Once confidence can be enhanced in submarine landslide signal detection  
50 and interpretation, passive seismic and acoustic sensing has strong potential to enable more complete  
51 hazard catalogues to be built, and opens the door to emerging techniques (such as fibre-optic sensing), to  
52 fill key, but outstanding, knowledge gaps concerning these important underwater phenomena.

53

## 54 **1. Introduction**

55 Submarine landslides can be orders of magnitude larger than those on land, occur on remarkably low  
56 angle (<2 degree) slopes, and can generate run-out that travels hundreds to thousands of kilometres into  
57 the deep-sea (Moore et al., 1989; Hampton et al., 1996; Nisbet and Piper, 1998; Piper et al., 1999; Carter  
58 et al., 2014). Underwater slope failures can generate tsunamis that inundate coastal communities that  
59 sometimes result in major loss of life (e.g. Harbitz et al., 2014; Tappin et al., 2014), and adversely impact  
60 critical seafloor infrastructure networks, such as the cables and pipelines on which we rely for global  
61 communications, the Internet, and energy supplies (Piper et al., 1999; Carter et al., 2014). To date, most  
62 studies of submarine landslides and their run-out have been based upon analysis of the deposits that past  
63 events left behind. These studies have used combinations of: i) seafloor surveys (e.g. multibeam  
64 echosounders and side scan sonars) to image submarine landslides in planform (e.g. Prior et al., 1982;  
65 McAdoo et al., 2000; Mountjoy et al., 2009; Casas et al., 2016; Normandeau et al., 2019; Brackenridge et  
66 al., 2020); ii) sub-surface geophysical surveys to determine the geometry and internal character of  
67 submarine landslide deposits (e.g. Gee et al., 2006; Bull et al., 2009; Vardy et al., 2012; Nwoko et al.,  
68 2020); iii) intrusive sampling or coring to calibrate geophysical interpretations, provide material for  
69 geochronological analysis (age and recurrence determination), and/or determine their source using  
70 geochemical and other analytical techniques (e.g. Geist and Parsons, 2010; Dugan, 2012; Urlaub et al.,  
71 2013; Vanneste et al., 2014); iv) in-situ or laboratory-based testing to understand geotechnical and  
72 geomechanical behaviour of submarine landslides (e.g. Sultan et al., 2010; Ai et al., 2014; Miramontes et  
73 al., 2018); v) analysis of ancient, exhumed submarine landslides from rock outcrops (e.g. Brookes et al.,  
74 2018; Bull et al., 2019; Ogata et al., 2019) and; vi) physical and numerical modelling to quantify slope  
75 stability, post-failure behaviour and resultant impacts (e.g. to seafloor infrastructure or the tsunami that  
76 they may initiate) (e.g. Sultan et al., 2010; Harbitz et al., 2014; Tappin et al., 2014; Puzrin et al., 2016).

77

78 These techniques provide valuable insights into the location, extent and nature of past failures, as well as  
79 providing the building blocks for generating models that enable inference of the likely behaviour of future  
80 events; however, they do not capture the behaviour of field-scale submarine landslides in action and do  
81 not reveal the in-situ conditions at the time of failure. Numerical models therefore remain relatively  
82 poorly constrained and many key questions remain unanswered; particularly with regards to the initiation,  
83 kinematics and impacts of submarine landslides. For instance, what are the preconditioning factors for  
84 failure and over what timescales are they important? Why are external triggers (e.g. earthquakes, tropical  
85 cyclones) more effective in some settings compared to others? What lag-times may be involved following  
86 cumulative or sudden perturbations that precede failure, and what controls that delay? Such information is  
87 critical to understand precisely how and when landslides are triggered and develop effective early  
88 warning systems, and to understand any climate change feedbacks (e.g. Maslin et al., 2004; Paull et al.,  
89 2007; Harbitz et al., 2014; Brothers et al., 2013; Normandeau et al., 2021). Key questions also remain  
90 unanswered on the kinematic behaviour of submarine landslides as they propagate. For example, what  
91 kinematics are involved during different styles of slope failure and how does that change as the mass  
92 travels down-slope? Why do some slopes fail suddenly, with major and rapid displacements, while others  
93 move much more slowly and progressively? Does failure type control the nature and extent of run-out,  
94 and if so, how? These, and many other, questions remain open, largely due to the challenges involved in  
95 monitoring failure processes and their precursor conditions in marine settings, in real time, that often  
96 cover very large areas.

97

98 Some of the challenges that inhibit monitoring of submarine landslides include:

- 99
- The *water depths* of many of the settings where submarine landslides occur place financial and  
100 logistical constraints on long-duration and continuous monitoring (e.g. Talling et al., 2013; Clare  
101 et al., 2017). While slope failures can occur in shallow water deltaic or fjord settings (e.g. Prior et  
102 al., 1989; Biscara et al., 2012), many occur in hundreds to thousands of metres water depth and  
103 have been documented in the deepest hadal trenches on Earth (Strasser et al., 2013; Kioka et al.,  
104 2019).

- 105 • The *remote nature* (i.e. location far from shore) of many submarine landslides provides  
106 constraints for power, communications and data transfer. This in turn limits the resolution and  
107 frequency of measurements that can be made due to a reliance on in-situ power supplies and  
108 recovery and redeployment of instruments by expensive vessels (Urlaub and Villinger, 2019).
- 109 • The *unpredictable nature of submarine landslides over time*. As many studies have suggested that  
110 submarine landslide recurrence may be Poissonian (i.e. approximately random), predicting when  
111 a specific seafloor slope may fail is a key challenge (Geist and Parsons, 2010; Urgeles and  
112 Camerlenghi et al., 2013; Urlaub et al., 2013). While relatively small (e.g. <1000 m<sup>3</sup>) submarine  
113 landslides might be relatively frequent (e.g. one or more per year) in high sediment-supply  
114 settings (e.g. fjord-head deltas), the events that pose a greater threat to seafloor infrastructure or  
115 are tsunamigenic (e.g. >>1 km<sup>3</sup>) tend to recur on much longer timescales (e.g. 100s->1000s of  
116 years). Continuous observations are required to capture these episodic events.
- 117 • The *large extent of areas affected by slope instability* means that monitoring at point-locations  
118 may completely miss events that occur elsewhere along the same margin (McAdoo et al., 2000;  
119 Urgeles and Camerlenghi et al., 2013; Casas et al., 2016; Collico et al., 2020; Gamboa et al.,  
120 2021). Being in precisely the right place at the right time is highly unlikely in all but a few  
121 settings where the controls on slope instability are well constrained (e.g. seasonally-active,  
122 spatially-focused sediment supply at steep submarine deltas; Lintern et al., 2016).
- 123 • The *powerful nature of the landslide and its run-out* poses a hazard to monitoring infrastructure  
124 that is placed in the way of a landslide (e.g. Inman et al., 1976; Khripounoff et al., 2003). Recent  
125 examples of field-based monitoring demonstrate how even relatively small flows can damage and  
126 displace sensors and associated equipment (e.g. Inman et al., 1976; Clare et al., 2020 and  
127 references therein). Large slope failures would likely completely destroy monitoring arrays in  
128 their path.

129

### 130 1.1. Recent advances in direct monitoring of submarine landslides

131 Despite these challenges, recent technological advances have enabled monitoring of several aspects of  
132 submarine landslide behaviour. Geotechnical monitoring provides information in relation to the  
133 preconditioning of submarine landslides, through use of in-situ devices that monitor changes in  
134 subsurface conditions, such as pore pressure (e.g. Prior et al., 1989; Strout and Tjelta, 2005; Stegmann et  
135 al. 2011). Technological advances have triggered a recent growth in geophysical monitoring of aspects of  
136 submarine landslides including: i) repeated seafloor surveys (at timescales from decades to minutes in  
137 some cases) to document elevation changes, evolution of the landslide itself, the effects of landslide run-  
138 out on the seascape, and subsequent reworking by other marine processes (e.g. Smith et al., 2007; Biscara  
139 et al., 2012; Kelner et al., 2016; Mastbergen et al., 2016; Fujiwara et al., 2017; Chaytor et al., 2020;  
140 Heijnen et al., 2020; Guiastrennec-Faugas et al., 2021; Normandeau et al., 2021); ii) time-lapse reflection  
141 seismic surveys to monitor changes in subsurface conditions (e.g. Blum et al., 2010; Hunt et al., 2021;  
142 Roche et al., 2021; Waage et al., 2021); (iii) direct monitoring of turbidity currents (some of which likely  
143 initiated from submarine landslides) using moored or vessel-based, active acoustic sensors, such as  
144 Acoustic Doppler Current Profilers (ADCPs) and multibeam sonars, that enable measurement of flow  
145 velocity and estimation of suspended sediment concentrations (e.g. Xu et al., 2010, 2011; Hughes Clarke  
146 et al., 2012; Khripounoff et al., 2012; Simmons et al., 2020); and iv) monitoring changes in seafloor  
147 movement and elevation via geodetic location of acoustic transponders (e.g. Campbell et al., 2015; Paull  
148 et al., 2018; Urlaub et al., 2018; Zhao et al., 2021). Such studies tend to involve either campaign-style  
149 surveys (often with years between individual campaigns), short duration (i.e. weeks to months-long)  
150 continuous measurements (as they are limited by power supply and data storage), or else require cabled  
151 connection for data transfer and external power supply. Therefore, while they provide detailed (i.e.  
152 temporally or depth/laterally-resolved) measurements, such approaches necessarily cover short time  
153 periods and limited areas relative to the full extent of continental slopes that may be affected by slope  
154 instability, as well as the extent of an individual landslide event itself (Urgeles and Camerlenghi et al.,  
155 2013; Urlaub and Villinger, 2019; Brackenridge et al., 2020; Fan et al., 2020). These studies also  
156 primarily focus on slope preconditioning, or the run-out produced by slope failures; hence, significant  
157 knowledge gaps remain with regards to the inception of slope failures, their kinematics, and their  
158 transition from slope failure to more dilute run-out, which are key, but poorly constrained parameters in

159 tsunami modelling, impact assessments for critical seafloor infrastructure, and in understanding deep  
160 water sediment transport in general.

161

## 162 **1.2. Aims**

163 There is thus a compelling need for low power-consumption sensors that can cover large spatial domains,  
164 which are capable of monitoring a wide range of environmental conditions (including the timing, location  
165 and behaviour of submarine landslides), and for systems that are deployed offshore to generate  
166 sufficiently small data volumes, such that sustained, long-endurance, autonomous monitoring is possible.  
167 Here, we show how passive acoustic and seismological monitoring has started to address these constraints  
168 and can contribute to filling key knowledge gaps. First, we explore the application of passive acoustic and  
169 seismological monitoring of terrestrial landslides, and the relevance of those techniques in the marine  
170 realm. Second, we discuss which aspects of submarine landslides may be detected using passive acoustic  
171 and seismological monitoring. Here, we explore the kinds of environmental noise or ground motion that  
172 are generated by submarine landslides, and therefore what signals we should anticipate recording. Third,  
173 we present examples from recent marine studies that have successfully monitored precursor conditions,  
174 initiation, movement and impacts of submarine landslides using passive acoustic and seismological  
175 approaches. Finally, we conclude with some of the on-going technological developments, and the future  
176 application of other techniques, including those detailed in other chapters of this volume.

177

## 178 **2. Passive geophysical monitoring of terrestrial landslides**

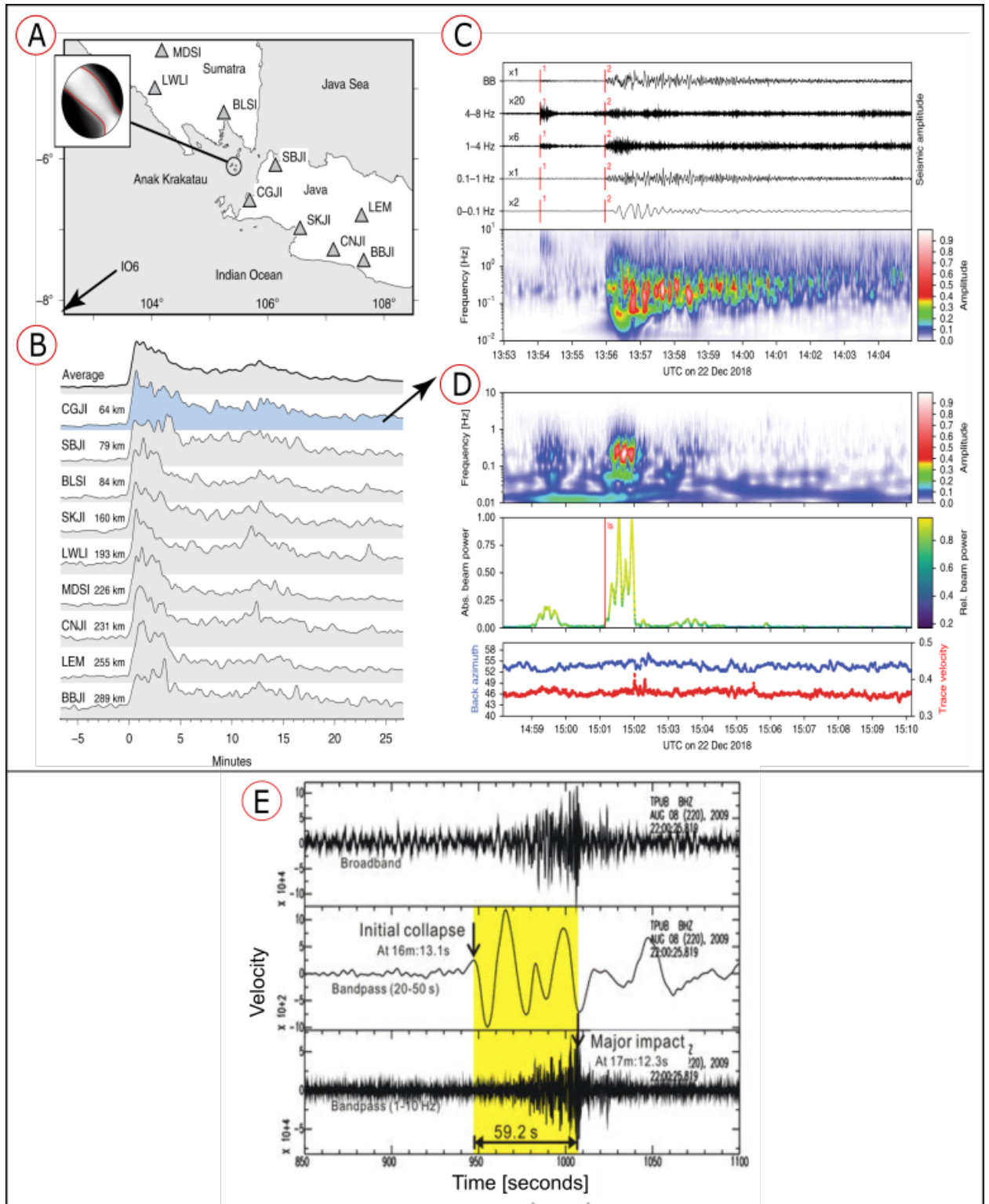
179 Early terrestrial studies successfully identified subsurface mining blasts and earthquakes using  
180 seismometers, which stimulated further research into the potential of passive geophysical monitoring to  
181 detect onshore slope failures (Galitzin, 1915; Jeffreys, 1923; Antsyferov, 1959; Cadman and Goodman,  
182 1967). The elastic straining of soils and rock, friction due to displacement along a failure plane, within the  
183 sliding mass, and collision of the landslide mass at its down-slope limit were subsequently recognised as  
184 signals that could be recorded by seismologic monitoring techniques (e.g. Cadman and Goodman, 1967).  
185 It is now well known that progressive failure and detachment of unstable masses can generate local  
186 ground motions that are equivalent to earthquakes; hence, land-based seismological networks are

187 increasingly used to determine the timing and location of slope failures, particularly in remote settings  
188 where repeat topographic surveys are rare or non-existent (e.g. Hibert et al., 2019). Such studies enable  
189 identification of many landslides that would otherwise be missing from historical records, thus providing  
190 significant improvements in the completeness of hazard catalogues (Ianucci et al., 2020).

191

192 In addition to creating ground motions, terrestrial landslide activity can also generate acoustic emissions,  
193 most of which tend to have a frequency content similar to, or just below, the spectrum of audible sound  
194 (Chichibu et al. 1989; Rouse et al. 1991; Dixon and Spriggs, 2007; Dixon et al., 2015). Acoustic  
195 emissions are generated as a slope is subjected to stress, shear and/or the landslide mass starts to move  
196 downslope (Dixon et al., 2015); hence, both acoustic emission and seismological monitoring have started  
197 to gain recognition as an onshore early warning tool to identify the early stages or precursors to slope  
198 failure (e.g. Mainsant et al., 2012; Dixon et al., 2015; Michlmayr et al., 2017; Le Breton et al., 2021).  
199 Analysis following the Anak Krakatau volcanic sector collapse in Indonesia (which generated a  
200 devastating tsunami in December 2018) revealed that broadband seismic and infrasound monitoring  
201 networks detected not only the landslide event, but also potential triggering events that preceded the  
202 collapse (Walter et al., 2019; Figure 1). Regional tsunami monitoring networks did not detect the resultant  
203 surface wave due to its localised point source, as they were designed to detect longer line sources (Ye et  
204 al., 2020). The collapse itself was represented by a short-lived (one to two-minute-long) low frequency  
205 (0.01-0.03 Hz) signal; the first P-wave of which was detected at nine onshore seismometers across the  
206 Sumatra and Java region, pin-pointing its location at Anak Krakatau (Walter et al., 2019; Figure 1). This  
207 event had a moment magnitude ( $M_w$ ) equivalent to 5.3. A higher frequency (0.1-4 Hz) seismic event was  
208 recorded 115 seconds prior to the sector collapse, while the collapse signal was followed by five minutes  
209 of a continuous tremor-like signal at high frequencies (0.7-4 Hz) that was attributed to post-failure  
210 eruptive activity. Infrasound arrays as far afield as Australia (>1000 km to the south-west) recorded a  
211 high-energy impulse that matched the origin times of the short-period seismic signal corresponding to the  
212 collapse event (Walter et al., 2019). This example is particularly pertinent, not only because it  
213 demonstrates the capability of passive seismological and acoustic monitoring to detect terrestrial

214 landslides onshore, but also because approximately half of the failed mass was actually under water (Hunt  
 215 et al., 2021).



216

217 **Figure 1: Seismic and infrasound records of the 2018 Anak Krakatau volcanic island collapse from**

218 **Walter et al. (2019), including: A) location of regional seismic monitoring network; B) vertical**

219 component of 0.4-1Hz seismic records at various stations; C) Normalised seismic amplitudes at the  
220 station nearest to Anak Krakatau recording a high frequency event prior to the collapse (1) and a  
221 low frequency signal that is related to the landslide (2); D) infrasonic spectrogram records of  
222 frequency, beam power and back azimuth used to locate the event from a seven-element infrasound  
223 array. E) Broadband seismogram (above), and band pass filtered by 20-50 seconds (middle) and 1-  
224 10 Hz as recorded before, during and after the 2009 Hsialin onshore landslide in Taiwan by Lin  
225 (2015).

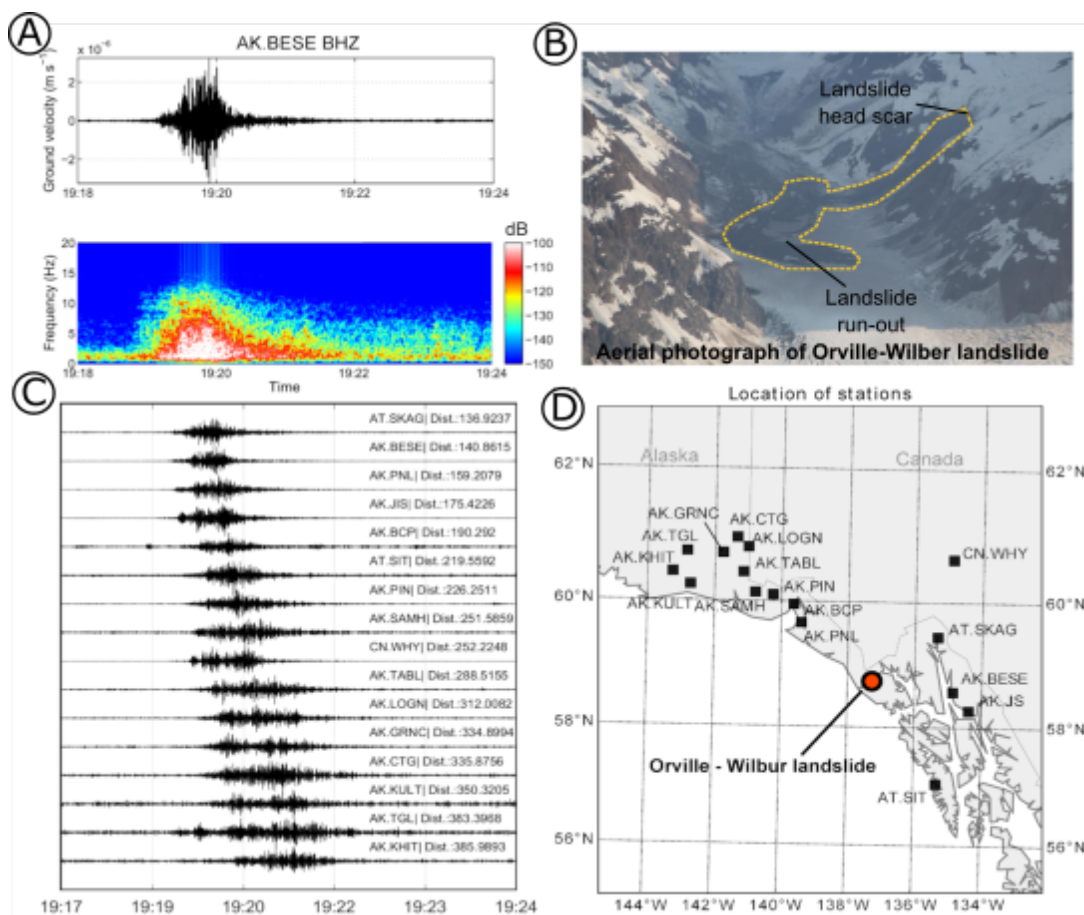
226

227 Onshore seismologic networks have been used to detect terrestrial landslides, including the Hsialin  
228 hillslope landslide, which occurred when Typhoon Morakot hit Taiwan in 2009. Broadband seismic data  
229 recorded: i) very long period seismic signals (20-50 seconds) that were interpreted to be related to elastic  
230 rebound of exposed stratigraphy as the overlying landslide mass was evacuated and moved downslope;  
231 and ii) large amplitude high frequency signals (1-10 Hz) that were interpreted to result from the impact of  
232 the landslide mass at the base of slope (Lin, 2015). Based on the time between these seismic events and  
233 the documented run out distance of 2,500 m, Lin (2015) estimated a maximum velocity of >80 m/s. A  
234 total of 51 other landslides were also detected on the same day by the same broadband network (Lin et al.,  
235 2010). Perhaps most remarkably, 14 of these were detected offshore. Hence, in instances where  
236 broadband seismic networks are sufficiently dense, they can provide a useful tool for hazard monitoring.

237

238 Processes that generate ground motion and create collisions within similar gravity-driven mass  
239 movements have also been successfully recorded using various passive geophysical techniques,  
240 including: i) submerged hydrophones and microphones to measure bedload transport based on noise  
241 generated by impacts caused by granular material in rivers and streams (Downs et al., 2016; Geay et al.,  
242 2017; Rickenmann, 2017; Geay et al., 2020); ii) bespoke geophone and infrasound arrays that detect self-  
243 generated noise and vibrations related to snow avalanches (Suriñach et al., 2005; Besson et al., 2007;  
244 van Herwijnen and Schweizer, 2011; Lacroix et al., 2012; Van Herwijnen et al., 2016); and iii) use of  
245 existing seismological stations to detect ice avalanches, rock falls and glacial outburst floods from sudden  
246 ground movements as the mass impacts the ground (Caplan-Auerbach and Hugel, 2007; Deparis et al.,

247 2008; Cook et al., 2018, 2021). The successful demonstration of passive geophysical tools to monitor  
 248 terrestrial mass movements has opened the door for the application of similar techniques in offshore  
 249 settings, with a view to overcoming some of the many shortcomings of active source monitoring tools  
 250 (e.g. particularly in relation to power and spatial limitations). Resolution and signal-to-noise ratio are  
 251 often orders of magnitude poorer for submerged instruments, as a result of: i) poor coupling with the  
 252 seafloor arising from their crude placement (i.e. where instrument frames are dropped from a ship, as  
 253 compared to the precise placement of instruments onshore; and ii) the environmental noise of the water  
 254 column, which is affected by a variety of natural processes and human activities.



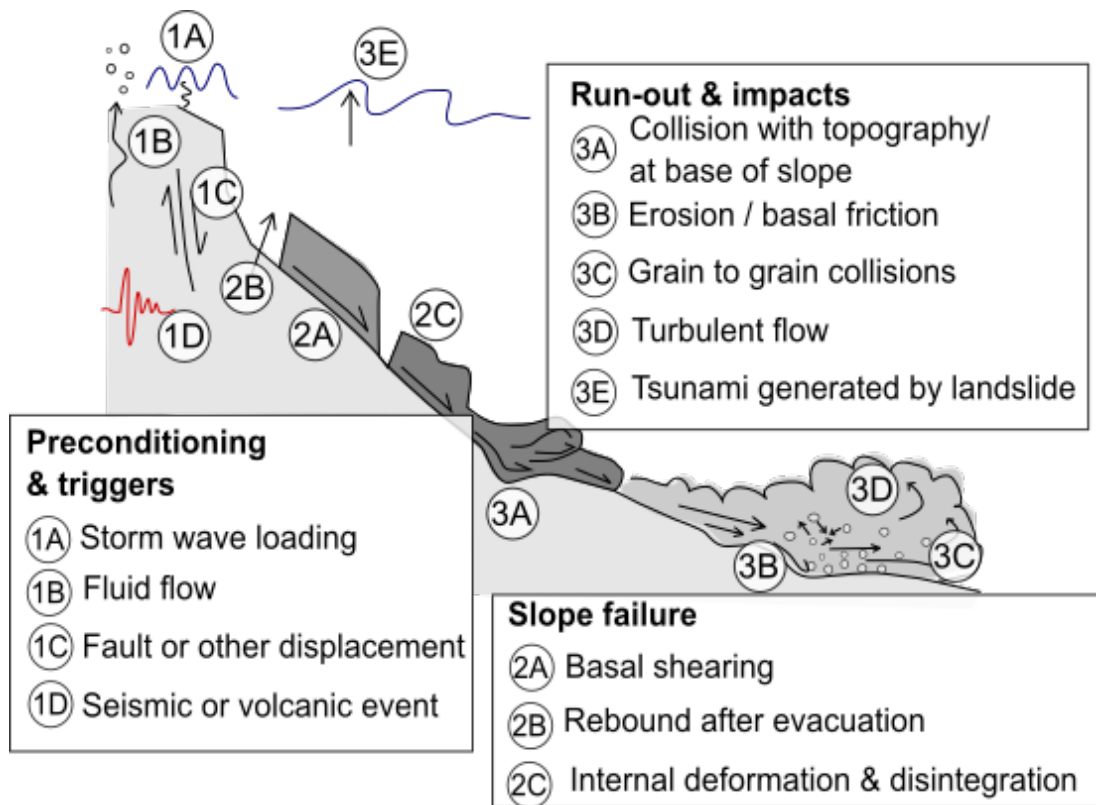
255

256 **Figure 2: Example of seismic records of terrestrial landslide, from Hibert et al. (2019), which was**  
 257 **detected by 17 stations between 136 and 385 km from the event itself. A) Seismic signal filtered**  
 258 **between 1 and 10 Hz. B) Aerial photograph of the landslide which provided the validation of the**  
 259 **signal interpretation. C) Seismic signals related to the same landslide at 16 locations, which are**  
 260 **shown in D) in relation to the landslide location.**

261 **3. Which aspects of submarine landslides should we be able to detect with passive systems?**

262 Based on these past studies, a range of information can theoretically be recorded from submarine  
263 landslides by passive seismic and acoustic monitoring (Figure 3). We now discuss some of these aspects,  
264 broadly in the order in which they would occur (i.e. prior to, during and then following a slope failure).  
265 First, data can be acquired in the build up to a slope failure, providing information on preconditioning,  
266 including temporal variations in volcanic or subsurface fluid flow activity, as well as potentially  
267 identifying any plausible external triggers such as earthquakes, tropical cyclones, storms or rapid  
268 sediment delivery by floods. Next, the timing and location of failure can potentially be ascertained by  
269 triangulating seismic signals (e.g. the case of the Anak Krakatau event), as a result of ground motions  
270 and/or noise generated as shearing occurs along the basal failure surface (and potentially also along its  
271 lateral margins), and as that shear propagates through the subsurface (Puzrin et al., 2016). As the  
272 landslide mass becomes mobile, ground motions and noise will likely be generated by friction created  
273 along the failure plane (Campbell et al., 1995; Brodsky et al., 2003; Gee et al., 2005), due to internal  
274 deformation of the moving sediment mass (e.g. Mountjoy et al., 2009; Buss et al., 2019; Sammartini et  
275 al., 2021), and if the mass starts to disintegrate as it entrains and mixes with ambient seawater (e.g.  
276 Masson et al., 2006). A reduction in vertical effective stress caused by evacuation of overlying sediments,  
277 or temporary loading and unloading as a result of the transit of an overriding landslide mass can trigger  
278 elastic rebound, producing long period signals (Kanamori and Given, 1982; Kawakatsu, 1989; Lin, 2015)  
279 that may occur suddenly, or steadily over prolonged timescales (e.g. >months in onshore examples; Lin,  
280 2015; Leung and Ng, 2016). The displaced mass that moves downslope may travel considerable distances  
281 (tens to hundreds of km), over relatively low angle (<1-2 degrees) slopes. The ground motions and noise  
282 generated will depend on the changing rheology and kinematics of that moving mass, and its interactions  
283 with the seafloor and any topography with which it encounters (e.g. Mountjoy et al., 2018). Friction  
284 arising from displacement and erosion at the base of the moving mass should be detectable, however the  
285 nature of the seafloor substrate may enhance or attenuate any signals that are generated. As the landslide  
286 disintegrates, it may switch from a plastically deforming mass of sediment, to a dense slurry dominated  
287 by grain to grain collisions, or a more dilute flow that is characterized by sediment suspended primarily  
288 by turbulence (e.g. Talling et al., 2007; Sumner and Paull, 2014; Paull et al., 2018). Each of these modes

289 will likely generate different signals. Where the moving mass generates a sudden physical impact and  
 290 comes to rest, such as at breaks in slope (ten Brink et al., 2006), following a sudden height drop  
 291 (Moernaut and De Batist, 2011), or where it meets pronounced topographic barriers (Frey-Martínez et al.,  
 292 2006), strong, high frequency signals should be anticipated (Caplan-Auerbach and Hugel, 2007; Deparis  
 293 et al., 2008). Finally, the indirect effects of the landslide may also generate a seismic signal, such as  
 294 where displacement of the overlying water mass generates a tsunami (e.g. Yuan et al., 2005).  
 295



296  
 297 **Figure 3: Schematic illustration of some aspects of submarine landslides capable of generating**  
 298 **seismic and/or acoustic noise as discussed in this chapter, relating to preconditioning and triggering**  
 299 **(1A-D), landslide inception and down-slope displacement (2A-C) and its subsequent evolution and**  
 300 **impacts (3A-E).**

301

#### 302 4. Recent advances and opportunities in passive monitoring of submarine landslides

303 Motivated by successful terrestrial landslide monitoring, and enabled by advances in offshore geophysical  
 304 monitoring (as highlighted by the other chapters in this volume and Baumgartner et al. 2018), several

305 recent studies have demonstrated that passive monitoring of several aspects of submarine landslides is no  
306 longer just a possibility, but a tangible reality. Many challenges remain; most notably the fingerprinting  
307 of seismic and acoustic signals. The paucity of direct submarine landslide monitoring studies (for reasons  
308 discussed earlier in this chapter) means that many of these signals remain poorly calibrated; hence,  
309 understanding the precise cause and source of signals is often unclear. That being said, recent studies  
310 have provided important forward steps in understanding previously unresolved aspects of submarine  
311 landslides and provide opportunities to fill other outstanding knowledge gaps. We now highlight studies  
312 that illuminate three of these areas: i) timing and location; ii) kinematics; and iii) run-out.

313

#### 314 **4.1. Determining the timing and location of submarine landslides at a margin scale using land-** 315 **based seismological networks**

316 Using networks of land-based seismological monitoring stations, seismic sources that did not correspond  
317 to catalogued earthquakes or storms have been located from radiating surface waves sourced in the Gulf  
318 of Mexico and the South China Sea. In the case of the Gulf of Mexico, 85 such non-earthquake seismic  
319 signals were identified between 2008 and 2015, located in various locations on the offshore continental  
320 slope, and have been attributed to submarine landslide activity (Fan et al., 2020; Figure 4). Individual  
321 landslide locations have previously been proposed from analysis of onshore seismological monitoring  
322 (e.g. Dewey & Dellinger, 2008; Ten Brink et al., 2008), but this is the first study to identify multiple  
323 submarine landslides. The seismic energy recorded is presumed to have arisen from the fast downslope  
324 movement of relatively rigid landslide masses (Fan et al., 2020). Given the density of offshore oil and gas  
325 infrastructure in the Gulf of Mexico (which is known to be vulnerable to damage by submarine landslides  
326 and their run-out), this study provides a much-improved understanding of the locations that are prone to  
327 slope failure (Chaytor et al., 2020). As well as identifying a number of seismic signals attributed to  
328 terrestrial landslides from an onshore broadband seismometer network, Lin (2015) also interpreted  
329 arrivals from offshore-generated ground motions in a region offshore SW Taiwan, to relate to submarine  
330 landslides, occurring shortly after the passage of the powerful Typhoon Morakot (8<sup>th</sup> August 2009). The  
331 triangulated location of these seismic sources was found to be clustered around submarine canyon flanks  
332 and steep continental slopes, which are known to be more prone to slope instability from previous

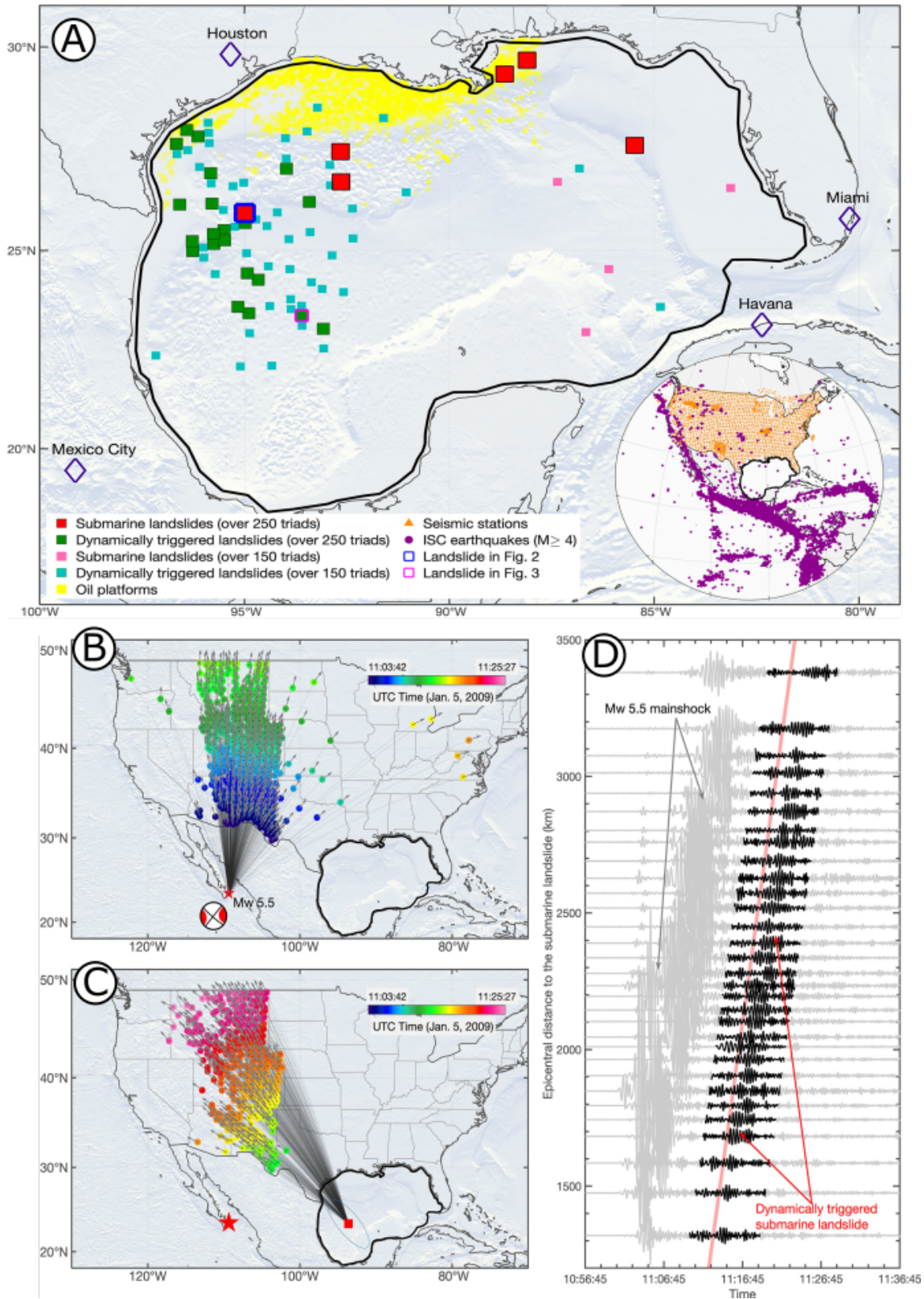
333 seafloor surveys (Yeh et al., 2021). Submarine sediment flows, that were likely triggered by slope failures  
334 and related to this event, damaged a number of telecommunications cables that crossed the Gaoping  
335 Canyon (Carter et al., 2014; Pope et al., 2017).

336

337 The ability to identify the timing and location of submarine landslides using existing onshore  
338 seismological networks (i.e. without the need for deployment of bespoke underwater sensors) offers a  
339 potentially game-changing opportunity to fill gaps in hazard catalogues that are required for the robust  
340 and resilient design of offshore engineering projects (e.g. oil and gas, renewables, subsea cables) and for  
341 developing hazard assessments for coastal communities (e.g. to inform tsunami warning and guide any  
342 related civil response planning). There is still a need to calibrate these interpretations through follow up  
343 seafloor surveys to document the true efficacy of the method and determine which landslide types are  
344 reliably detected. Indeed, Fan et al. (2020) point out that this approach will likely only detect landslides  
345 that generate sufficient seismic energy; hence, slow (e.g. creep-like) or small landslides are unlikely to be  
346 detected. While submarine landslide catalogues may become more extensive using this method, they will  
347 remain incomplete for such events that do not generate discernable seismic noise. Given the fact that  
348 tsunamigenic landslides tend to be faster and larger, this method therefore provides a very promising step  
349 forward in submarine landslide detection across very large areas, and will only be strengthened as  
350 broadband seismic networks are expanded. A further positive is that these passive detection methods  
351 provide a low cost approach to tackle the current biases in submarine landslide studies, given that the  
352 majority of these presently focus on the North Atlantic and offshore from more economically developed  
353 countries (Clare et al., 2019).

354

355



356

357 **Figure 4: Identification of submarine landslides using terrestrial seismometer networks from Fan**  
 358 **et al. (2020). A) Locations of seismic signals interpreted to relate to submarine landslides in the**  
 359 **Gulf of Mexico using the onshore seismic monitoring network. Inset shows earthquakes in the**

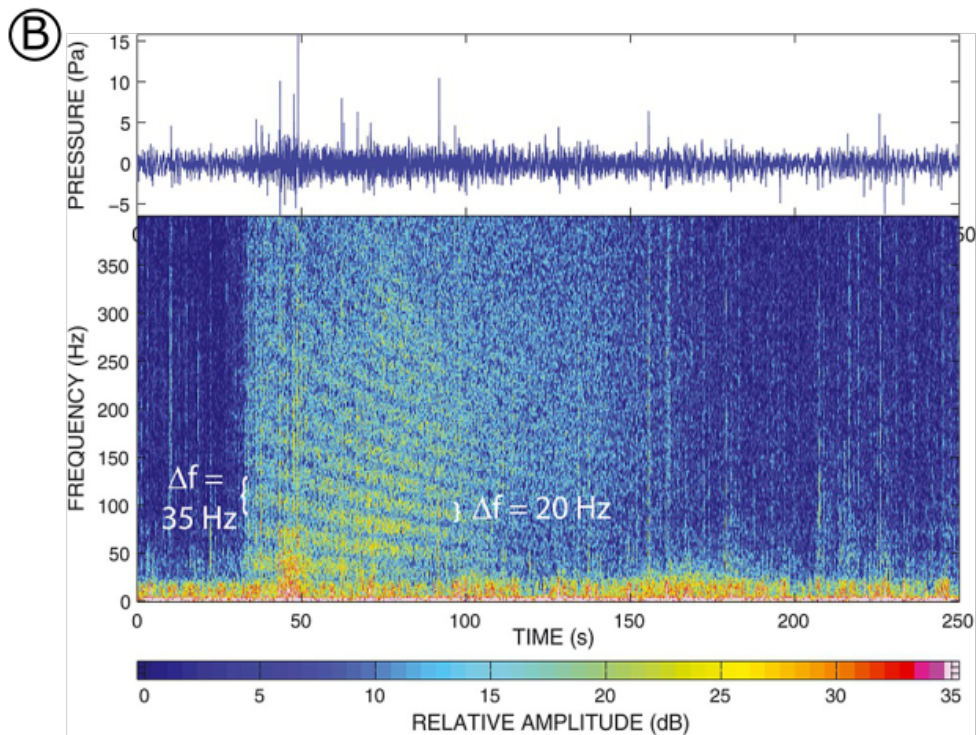
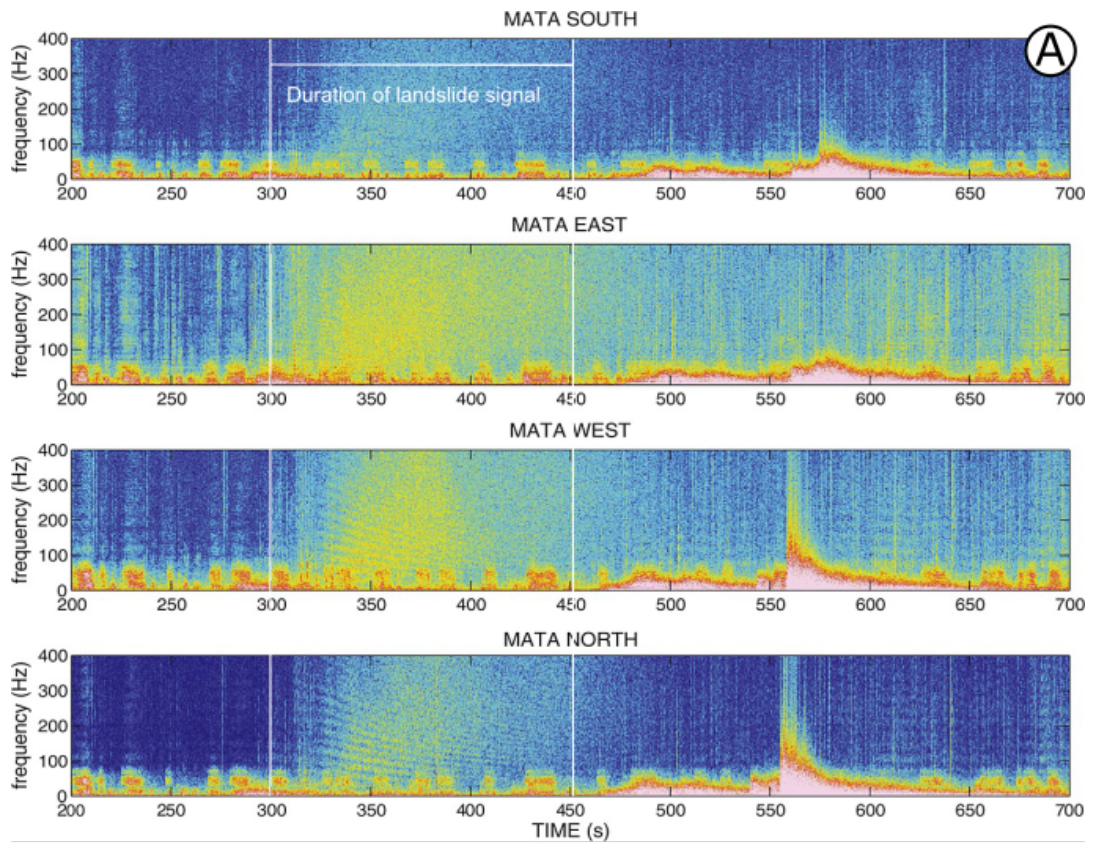
360 **monitored time period (2008-2015) of magnitude 4 or above. B) Rayleigh wave arrival times**  
361 **(colours of circles) and propagation directions (lines) for an earthquake, and C) a submarine**  
362 **landslide that is thought to have been triggered by that same earthquake (red star). D) Bandpass**  
363 **filtered (20-50 seconds) waveforms for a selection of the seismic stations used to locate the**  
364 **submarine landslide. Grey signals show precursor earthquake and black shows the signal of the**  
365 **landslide itself.**

366

#### 367 **4.2. Quantifying landslide kinematics using hydrophones**

368 Submarine landslide-generated noise has been used to determine the existence of events in remote  
369 oceanic settings that would otherwise have likely gone unnoticed. Networks of hydrophones, including  
370 the Hawaii Undersea Geo-Observatory in the Pacific Ocean, recorded a combination of partly-subaerial  
371 and fully-submarine landslides on the flanks of volcanic islands, which generated acoustic signals that  
372 were recorded up to 7000 km from their source; sometimes exceeding the amplitudes generated by  
373 volcanic eruptions by up to an order of magnitude (Caplan-Auerbach et al., 2001; Chadwick et al., 2012;  
374 Caplan-Auerbach et al., 2014; Figure 5). The distinctive, extremely low frequency signals recorded are  
375 thought to relate to the collapse of large landslide blocks, composed of highly competent volcanic  
376 material, as well as from their disintegration as they travelled downslope as an avalanche (Chadwick et  
377 al., 2012). In these instances, the triggering event generally seems to relate to enhanced volcanic activity,  
378 such as at the West Mata volcano near Tonga, and at Kilauea volcano, Hawaii (Caplan-Auerbach et al.,  
379 2001; 2014). In addition to pinpointing their location, and identifying the timing relative to volcanic  
380 activity, the multi-pathing of the propagated sound waves enabled determination of the landslide transit  
381 velocities, which are estimated at between 10 and 25 m/s (Caplan-Auerbach et al., 2014). The location (in  
382 particular the water depth) of a landslide source, and its initial velocity, are key inputs for tsunami  
383 modelling (e.g. Løvholt et al., 2015). Typically, these parameters remain poorly or entirely un-  
384 constrained, which results in a wide uncertainty in any predictive tsunami modelling. Therefore, these and  
385 future observations using similar hydrophone networks can play an important role in improving our  
386 understanding of a globally significant hazard (e.g. Tappin et al., 2008; Harbitz et al., 2014; Goff and  
387 Terry, 2016). Again, calibration of the hydrophone signals is needed; hence, field studies that make multi-

388 parameter measurements of submarine landslide activity will contribute significantly to the fingerprinting  
389 of different acoustic responses, and will enhance confidence in the future acoustic detection and  
390 characterization of submarine landslides.  
391



392

393 **Figure 5: Hydrophone spectrograms showing evidence of submarine landslides in the SW Pacific**  
394 **from Caplan-Auerbach et al. (2014). A) The signal between 300 and 450 seconds is interpreted as a**  
395 **submarine landslide due to its broadband spectrum and variable frequency content. It is distinct**  
396 **from degassing explosions (low frequency, <50 Hz) events and regional earthquakes (very low**  
397 **frequency between 470 and 600 seconds). B) Hydrophone time series and spectrogram for a**  
398 **submarine landslide. Interference bands are noted – at 35 Hz at the start of the landslide and 20 Hz**  
399 **near the end. The change in spacing of frequency bands indicates a moving source and is used to**  
400 **infer the vector velocity of the landslide.**

401

#### 402 **4.3. Characterising landslide run-out to enhance hazard assessments**

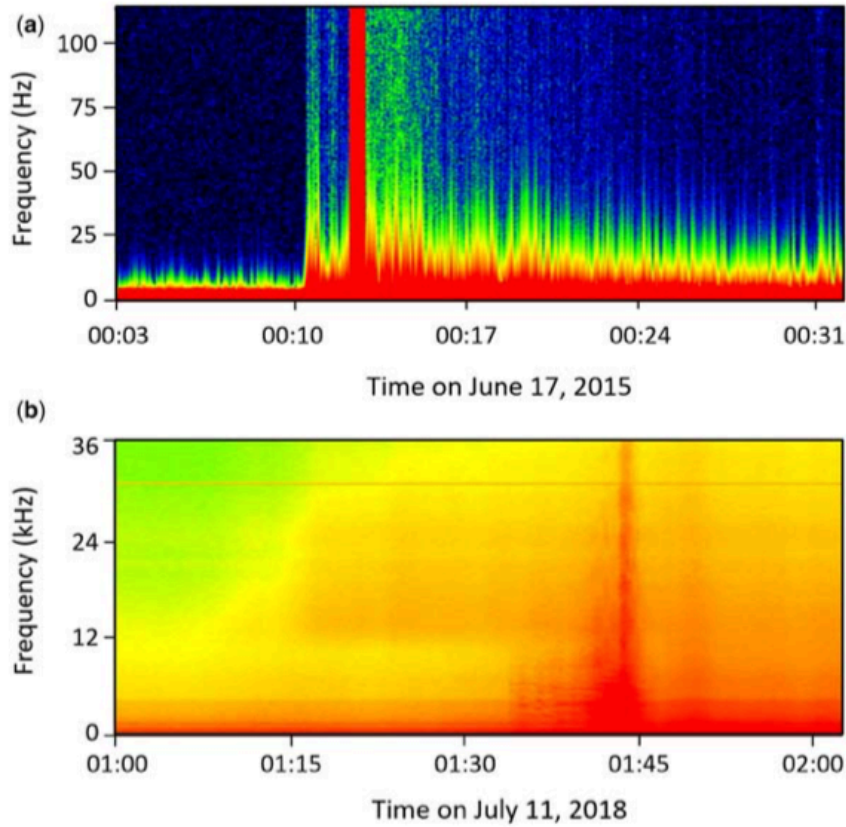
403 Submarine landslide run-out is often far more extensive than that on land, and may evolve dramatically  
404 with regard to its rheology, as flows mix with seawater and/or entrain seafloor sediment (Parker, 1982;  
405 Zeng et al., 1991; Mohrig and Marr, 2003; Gee et al., 2006; Heerema et al., 2020). As these mass flows  
406 can travel at high speeds and across large distances, they can damage sensors placed in their path (e.g. see  
407 several examples in Clare et al., 2020). Therefore the use of passive, remote sensing acoustic and seismic  
408 monitoring tools, placed out of the direct pathway of such flows, can enable undisturbed monitoring and  
409 reduce instrument damage or loss. Recent studies have demonstrated how hydrophones may record  
410 turbidity currents (some of which were triggered by landslides) in fjord settings that are fed by seasonally  
411 active rivers, including on the Fraser and Squamish deltas; both in British Columbia (Lintern et al., 2016;  
412 2019; Hizzett et al., 2018; Hay et al., 2021; Figure 6). At the Fraser Delta, hydrophones are deployed on a  
413 seafloor observatory that is connected to shore via the VENUS cabled network, enabling real-time  
414 streaming of data, which also includes measurements by complementary active source geophysical  
415 sensors (Lintern and Hill, 2010). Sensors such as Acoustic Doppler Current Profilers, provide the  
416 calibration and confidence that the acoustic signals (which include both high (1-300 kHz) and low (Hz)  
417 frequency ranges) can be attributed to turbidity currents (Lintern et al., 2016; 2019). At the Squamish  
418 Delta, a hydrophone suspended from a vessel, 10 m above an active submarine channel, recorded the  
419 noise generated from sixteen turbidity currents that reached speeds of 2 m/s (Hay et al., 2021). Extensive  
420 calibration was provided by a pair of 500 kHz multibeam sonars placed on the same frame as the

421 hydrophone, three echosounders (28, 200 and 70-110 kHz) mounted on the vessel itself, and a 1200 kHz  
422 ADCP suspended from a separate frame, also 10 m above the seafloor (15 m from the hydrophone  
423 frame). This novel study showed that where turbidity currents exceeded 1 m/s, they generated noise well  
424 above ambient ocean conditions, across a spectrum of 10-500 kHz; interpreted to result from highly  
425 energetic sand-sized particle collisions. Cross-reference of hydrophone and ADCP-derived velocity  
426 measurements, revealed that spectral density (at 100 kHz frequencies) is proportional to the speed of the  
427 flow front, where a 100-fold increase in spectral density relates to a doubling in frontal speed (Figure 7;  
428 Hay et al., 2021). Even more powerful sediment flows (i.e. >2 m/s, and potentially >10 m/s) that occur  
429 within larger submarine canyons and channels (e.g. Carter et al., 2014; Azpiroz et al., 2017; Paull et al.,  
430 2018), or that travel vast distances across open continental slopes (e.g. Piper et al., 1999), may generate  
431 similar acoustic signals, and/or are likely to also generate ground motions (depending on their velocity,  
432 interaction with, and the nature of the surrounding topography and seafloor substrate) that can be detected  
433 with seismometers, but this requires future investigation.

434

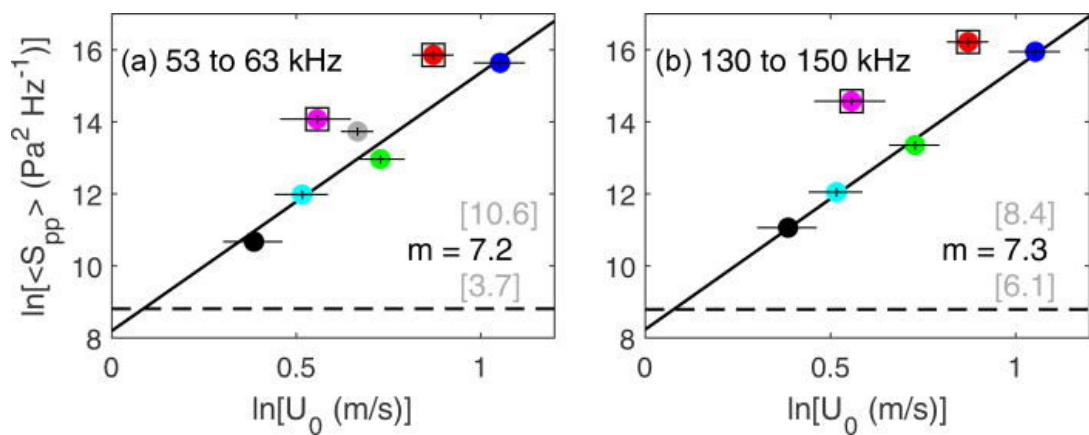
435 Seafloor cabled-networks, such as the Neutrino Mediterranean Observatory-Submarine Network 1  
436 (NEMO-SN1), have demonstrated that offshore seismic monitoring can also play a future role in  
437 detecting the run-out from submarine landslides. While background environmental noise was often found  
438 to complicate conclusive signal identification, high frequency and long duration (at least longer than that  
439 of earthquakes) signals recorded by an ocean bottom broadband seismometer on the NEMO-SN1 network  
440 offshore Mount Etna were attributed to submarine landslide run-out (Sgroi et al., 2014). Therefore, this  
441 approach can apparently be readily applied using marine seismometer networks, and similar deployment  
442 of more than one seismometer would allow for greater characterization of events, including pin-pointing  
443 their source. These recordings were of particularly high quality because the dedicated installation  
444 procedure using a Remotely Operated Vehicle ensured excellent coupling with the seafloor. This is not  
445 always the case for Ocean Bottom Seismometer surveys, as these instruments are typically dropped from  
446 a surface vessel and land in a relatively uncontrolled manner on the seafloor.

447



448

449 **Figure 6: Hydrophone spectrograms showing turbidity current events in British Columbia. (a)**  
 450 **Passing directly through a hydrophone at the delta dynamics laboratory at the Fraser Delta. (b)**  
 451 **Passing below a mooring in the Bute Inlet Channel, British Columbia from Lintern et al. (2019).**



452  
 453

454 **Figure 7: Cross-comparison of band-averaged noise spectral densities ( $S_{pp}$ ) with frontal velocities**  
 455 **( $U_0$ ) of turbidity currents recorded in the Squamish Delta, British Columbia for two frequency**  
 456 **bands (from Hay et al., 2021). Coloured symbols represent different turbidity current events. Solid**

457 **black line is a best-fit trend and the dashed black line shows the detection threshold above ambient**  
458 **noise levels.**

459

#### 460 **4.4. Opportunities using distributed cable-based sensing**

461 Spatially-resolved distributed sensing along seafloor fibre-optic cables now enables broadband seismic  
462 and acoustic monitoring across long distances (over 10s-100s of km). Several recent studies have  
463 demonstrated temporally- and spatially-resolved monitoring of ground motion (acting like distributed  
464 networks of seismometers) generated by earthquakes, fault displacements, and acoustic noise created by  
465 ocean waves and deep-sea bottom currents that resuspend sediment at the seafloor (e.g. Blum et al., 2010;  
466 Marra et al., 2018; Ajo-Franklin et al., 2019; Lindsey et al., 2019; Williams et al., 2019; Zhan et al., 2020;  
467 Nishimura et al., 2021; Zhan et al., 2021; Wilcock, 2021; Figure 8). Distributed acoustic sensing data  
468 acquired along a fibre-optic cable in the Nankai subduction zone, western Japan, was found to have a  
469 comparable performance to adjacent broadband ocean bottom seismometers at seismic frequencies of >1  
470 Hz, provided the cable was well-coupled to the seafloor (Ide et al., 2021). The same study concluded that,  
471 even though such distributed acoustic monitoring records one component of strain, seismic source  
472 localisation within tens of kilometres of the cable can still be achieved. At lower frequencies (i.e. 0.02-  
473 0.05 Hz) the distributed acoustic sensing observations were notably noisier compared to those from ocean  
474 bottom seismometers, thus making detection of such events challenging, unless events occur very close to  
475 the cable. The low frequency regime may be critical regional scale landslide detection (i.e. Fan et al.,  
476 2020); hence this technique may be most appropriate for detecting relatively local low or far-field high  
477 frequency signals, but more studies are required that provide similar comparisons, to test the sensitivities  
478 of different cable configurations, interrogator units and analytical approaches (Lindsey and Martin, 2021;  
479 Lior et al., 2021).

480

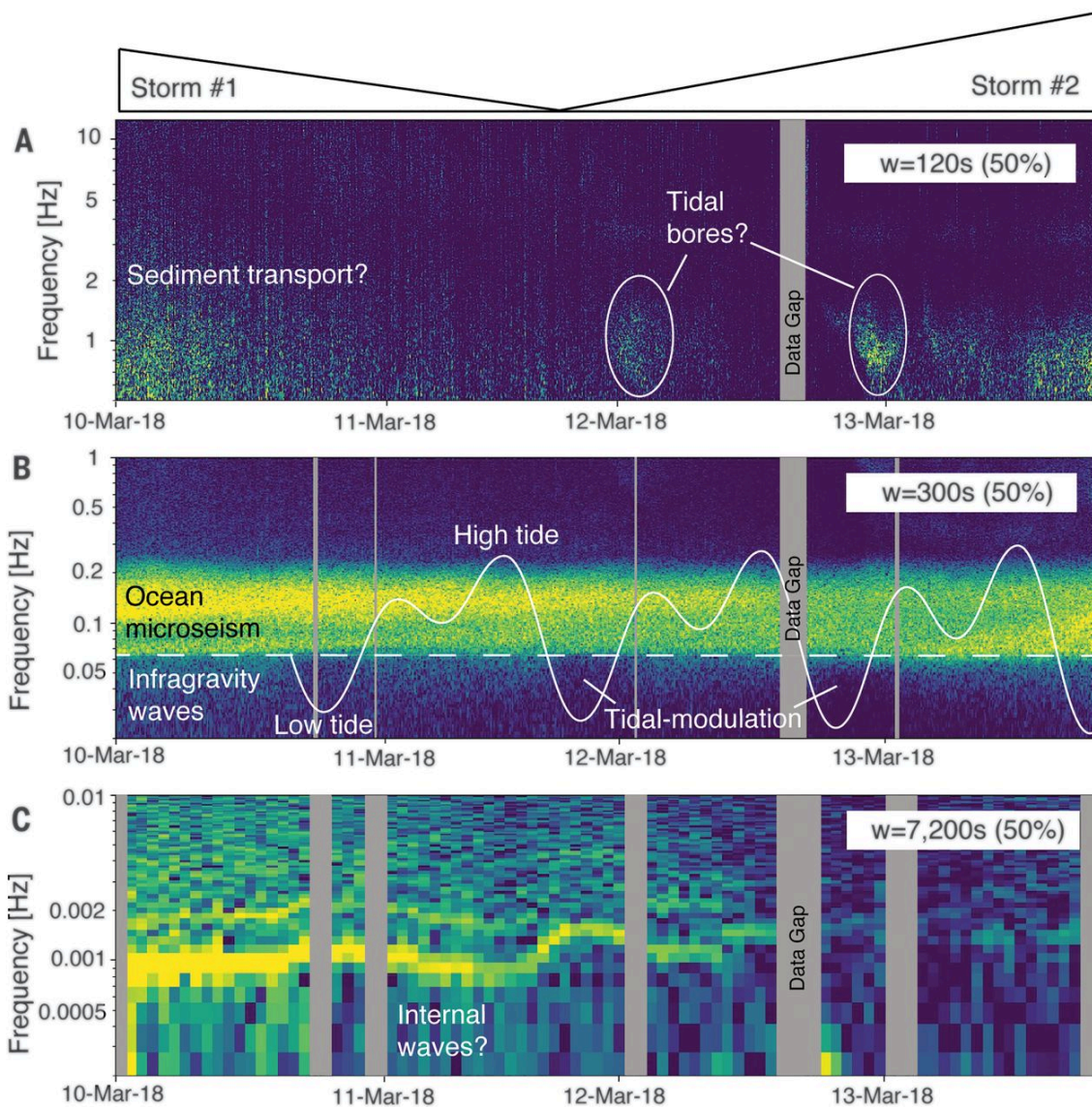
481 Recent advances have seen the application of sensing to detect changes in the State of Polarisation over  
482 the full length of a 10,000 km-long telecommunications cable, which enabled recording of moderate to  
483 large earthquakes, as well as pressure signals from ocean swells (thus illustrating the potential for real-  
484 time tsunami detection over transoceanic distances; Zhan et al., 2021). This distance far exceeds that

485 reached by previous studies and did not require specialist interrogator units or ultra-stable laser sources;  
486 instead monitoring the State of Polarisation to detect anomalies that are attributed to strong seismic waves  
487 or long-period water waves (Zhan et al., 2021). It should be noted, however, that these long-range  
488 measurements were spatially integrated (i.e. averaged along the entire fibre length); hence, additional,  
489 independent information is required to locate and further characterise the hazard, besides the locally-  
490 recorded signal timing and magnitude. Zhan et al. (2021) also recognised that site-specific effects can  
491 affect the sensitivity of measurements, wherein the seabed coupling and nature of the seabed substrate on  
492 which the cable is placed can result in spatially variable signal attenuation. Indeed, the coupling of the  
493 cable with the seafloor may be particularly important for cable-based sensing. When assessing the  
494 efficacy of Distributed Acoustic Sensing to detect earthquakes, Lioer et al. (2021) found that performance  
495 was notably reduced in areas of highly irregular, rocky seafloor, where the cable is locally in free span,  
496 raised above the seafloor across sections, and enhanced in areas of low relief, soft seafloor, particularly  
497 where cables may become embedded or buried by sedimentation. Going forwards, cable sensing is likely  
498 to be complimentary to other approaches, but also has strong potential to fill in major geographic gaps in  
499 seismic monitoring, potentially making use of the existing global network of submarine cables and  
500 accessing new cables (Ranasinghe et al., 2018; Howe et al., 2019; Mizutani et al., 2020; Mecozzi et al.,  
501 2021; Wilcock, 2021).

502

503 While Distributed Acoustic Sensing can provide valuable information, such sensing is limited to no more  
504 than a few hundred km from shore; hence, additional sensors, that could include hydrophones or  
505 geophones, distributed at nodal locations along a cable may help to fill this gap over longer distances.  
506 This is the premise of the SMART (Science Monitoring and Reliable Telecommunication) Cables  
507 initiative, which proposes attaching instruments, including ground motion, pressure and temperature  
508 sensors, as external nodes on repeaters (typically spaced 60-80 km apart) on new or decommissioned  
509 submarine telecommunication cables (Ranasinghe et al., 2018; Howe et al., 2019; Mecozzi et al., 2021).  
510 The CAM (Continent-Azores-Madeira) Ring cable is likely to be the first operational SMART Cable  
511 system (coming online in 2024), connecting mainland Portugal with the Azores. As these nodes are  
512 powered and connected by cables, they will potentially provide opportunities for real-time seismo-

513 acoustic monitoring far from shore. This is particularly relevant for the CAM Ring cable, as the strongest  
 514 earthquakes occur far offshore, and many of the previously mapped submarine landslides are located on  
 515 the flanks of remote submerged seamounts (Gamboa et al., 2021; Matias et al., 2021). Numerical  
 516 modelling indicates that the CAM Ring SMART cable should significantly reduce uncertainty in  
 517 pinpointing the location and timing of offshore earthquakes and identify events (such as submarine  
 518 landslides) that are currently undetectable by the existing onshore and coastal monitoring networks, while  
 519 detection of the passage and direction of tsunamis should provide improved early warning of coastal  
 520 impacts, and thus time to prepare emergency responses (Matias et al., 2021).



521

522 **Figure 8: Frequency spectrograms from Distributed Acoustic Sensing along a seafloor fibre optic**

523 **cable offshore Monterey Bay, California from Lindsey et al., 2019. These demonstrate how this**

524 **technique can be used to detect: A) short-lived tidal and near-bed currents; B) tidal effects due to**  
525 **pressure changes; C) and internal waves. Therefore, this approach may also be appropriate to**  
526 **measure aspects such as the run-out of submarine landslides (e.g. turbidity currents), displaced**  
527 **water masses in front of a moving mass or ground motions generated by the landslide itself.**

528

## 529 **5. The application of passive geophysical monitoring in advancing submarine landslide science**

530 We now revisit the overarching challenges and science questions that were outlined in the introductory  
531 section, specifically addressing how emerging seismic and acoustic techniques can fill outstanding  
532 knowledge and capacity gaps, which uncertainties remain, and outline a proposed strategy for the forward  
533 steps to advance submarine landslide science.

534

### 535 **5.1. Can passive seismic and acoustic techniques overcome the logistical challenges that have** 536 **previously-hindered monitoring of submarine landslides?**

537 First, we respond to the logistical challenges; namely the often-deep water and remote location of  
538 submarine landslides, and their unpredictable and powerful nature. Provided sensors and receivers are  
539 protected in appropriate pressure housing, passive seismo-acoustic landslide monitoring using  
540 hydrophones and geophones can be performed across the full range of water depths in the global ocean,  
541 from coastal (e.g. Hay et al., 2021) to thousands of metres water depth (e.g. Caplan-Auerbach et al.,  
542 2014). To date, we are not aware of any landslide monitoring in hadal water depths, but it is certainly  
543 logistically possible, and the use of ocean bottom seismometers and Distributed Acoustic Sensing along  
544 fibre-optic cables is increasing in many deep ocean settings to record earthquake and non-earthquake  
545 related noise (e.g. >4000 m offshore Chile, Batsi et al., 2019; Ide et al., 2021). Given the relatively early  
546 stages of many the techniques we have described, most previous studies have relied upon individual  
547 instruments, or limited networks of seabed or moored instruments, with narrow spatial coverage. Hence,  
548 widespread (i.e. basin- to ocean-scale) passive monitoring of submarine landslides very much remains an  
549 open and future challenge. However, onshore seismic monitoring networks are far more dense than those  
550 offshore and, where margin geometry permits, these can immediately be used to identify submarine

551 landslides that may occur hundreds to thousands of kilometres from shore, where their location is not  
552 known *a priori* (Fan et al., 2020).

553

554 The Gulf of Mexico is perhaps an ideal candidate, as its physiographic geometry suits the use of  
555 triangulation from an onshore network to pinpoint the offshore location of submarine landslides. Arc-  
556 shaped convergent continental margins are also good future candidates for this approach, as are enclosed  
557 basins such as the Mediterranean, as they provide similarly well-suited geometries, and are often  
558 themselves ‘blind spots’ for landslide-tsunami hazard where new insights are required (e.g. Sunda Arc;  
559 Goff and Terry, 2016). The geometry of many margins will not suit this approach, however. As  
560 recognised by Lin (2015), deployment of wider and denser networks of onshore and offshore  
561 seismometers will be required in such settings for limitations to be overcome. Distributed Acoustic  
562 Sensing along fibre-optic cables provides opportunities for long distance monitoring, and potentially to  
563 fill several spatial gaps in offshore monitoring capacity, however, this technology cannot currently be  
564 extended beyond the first repeater, and is thus presently limited over distances of less than a few hundreds  
565 of kilometres from shore (Matias et al., 2021). This means that many submarine landslides, which occur  
566 far offshore, cannot yet be recorded by this technique. Longer range (i.e. tens of thousands of kilometres)  
567 monitoring is possible along cables that connect continents, either as integral measurements with limited  
568 spatial resolution (e.g. Marra et al., 2018; Zhan et al., 2021), or at powered SMART sensor nodes along  
569 the cable (e.g. Howe et al., 2019).

570

571 All of the passive monitoring approaches enable placement of sensing equipment out of the path of  
572 submarine landslides and their run-out, which has hindered many previous efforts where sensors,  
573 moorings and platforms have been damaged or lost (e.g. Khripounouff et al. 2003; Clare et al., 2020 and  
574 references therein). These new techniques therefore ensure that not only the timing initiation of a  
575 landslide can be recorded, but measurements can also be made during the landslide event itself, from  
576 which key aspects of landslide behaviour can be determined.

577

578           **5.2. Which aspects of submarine landslides can we currently assess from passive remote sensing**  
579           **techniques and what needs to be resolved?**

580   **5.2.1. Landslide timing**

581   The timing of submarine landslides has been determined from signals detected by submerged  
582   hydrophones and geophones, as well as land-based seismic monitoring systems. Therefore, observational  
583   passive monitoring datasets can provide new insights into the timing and frequency of submarine  
584   landslides; starting to fill a key knowledge gap. For example, the use of land-based seismic monitoring in  
585   the Gulf of Mexico identified 85 previously-undetected submarine landslide events (Fan et al., 2020). The  
586   ability to identify past submarine landslide signals provides important information to develop more robust  
587   hazard assessments and inform resilient routing and siting of offshore infrastructure (Chaytor et al.,  
588   2020), while the quick identification of landslide signals has potential to enhance existing tsunami  
589   warning systems (Fan et al., 2020; Matias et al., 2021). An immediate opportunity lies in back-analysis of  
590   legacy datasets, to explore whether past landslide signals exist, but have been ignored by previous studies  
591   as they focused on different frequency spectral ranges. Such an approach has already shown value in  
592   identifying gas or fluid flow-related processes from ocean bottom seismometers or ocean currents from  
593   Distributed Acoustic Sensing datasets (Baksi et al., 2019).

594

595   **5.2.2. Landslide triggers and preconditioning**

596   In addition to determining whether a landslide has occurred or not, ascertaining the timing of landslide  
597   inception allows us to investigate the environmental conditions in the build up to that event; and thus  
598   determine likely triggering and/or preconditioning factors. Limitations in the precise determination of  
599   submarine landslide timing (e.g. due to uncertainties in radiocarbon dating) has hindered identification of  
600   these links previously, but this is now possible, as highlighted by acoustic and seismic monitoring prior of  
601   the 2018 Anak Krakatau volcanic collapse (Walter et al., 2019) and offshore landslides following  
602   earthquakes in Taiwan (Lin, 2005). Future monitoring is likely to lead to the identification of new or  
603   potentially surprising triggers, such as the intriguing link between distant earthquakes and submarine  
604   landslides in the Gulf of Mexico (Fan et al., 2020). Passive monitoring technology is now sufficiently  
605   mature to test previous hypotheses on landslide triggering and investigate new ones; however, operational

606 early warning systems (i.e. that automatically raise alerts ahead of a potential landslide event) still  
607 remains a future prospect for all but a few locations, as this requires a robust understanding of the  
608 conditions prior to failure or identification of a landslide as it happens. This will therefore be more  
609 feasible at sites where triggers and/or preconditioning are more predictable and closely linked to  
610 enhanced sediment supply from rivers (i.e. where landslides are more prone during or following periods  
611 of higher river discharge, such as the bedload-dominated Fraser or Squamish Delta; Lintern et al., 2020;  
612 Hay et al., 2021) or relate to heightened volcanic activity (e.g. Anak Krakatau, Indonesia; Mount Etna,  
613 Mediterranean; Urlaub et al., 2018; Walter et al., 2019).

614

### 615 **5.2.3. Landslide location**

616 It is possible to pinpoint the location of submarine landslides through triangulation (to a precision of  
617 approximately tens of kms; Caplan-Auerbach et al., 2014; Lin, 2015; Fan et al., 2020); however, as  
618 already noted, this approach is limited to locations where sensor networks are sufficiently widely and  
619 densely distributed. There is a wealth of existing onshore (and to a limited extent offshore) broadband  
620 seismic datasets in several regions where the same approach could be taken, to investigate whether  
621 similar landslide-like signals exist, if they can be located spatially, and if they correspond to any of the  
622 recent direct measurements of slope instability and their run-out, or existing maps of landslide  
623 vulnerability (e.g. Paul et al., 2018; Urlaub et al., 2018; Obelcz et al., 2020; Gamboa et al., 2021). We  
624 suggest that detailed bathymetric surveys should be performed in areas where seismic signals attributed to  
625 submarine landslides have been located to determine which types of landslide are recorded, as well as to  
626 test the efficacy of landslide detection. The Gulf of Mexico, Mediterranean, Caribbean and regions  
627 offshore south-west Taiwan are prime candidates for this field calibration.

628

### 629 **5.2.4. Landslide kinematics**

630 If a landslide mass is known, it is possible to infer other aspects of submarine landslide behaviour from  
631 the resultant seismic and acoustic signals. For instance, inversion of these signals can be used to derive  
632 force histories, from which volume, velocity, changes in basal friction, run-out distance, and other  
633 important aspects of landslide kinematics can be determined, as demonstrated by successful application of

634 these approaches in terrestrial settings (e.g. Brodsky et al., 2003; Ekström and Stark, 2013; Yamada et al.,  
635 2013; Moretti et al., 2015). These aspects will likely be more challenging to constrain than landslide  
636 timing and location, however; requiring concerted research and field calibration. Sites where passive and  
637 active monitoring are performed concurrently will provide valuable opportunities to calibrate the nature  
638 of seismic and/or acoustic signals, such as at the Squamish Delta, Canada, where variations in noise  
639 spectra were linked to changes in the concentration and grain size of sediment avalanches, and noise  
640 intensity corresponded to the velocity of the flow front of turbidity currents (Hay et al., 2021). Moored  
641 arrays of direct active sensors (e.g. ADCPs) have been used to track the passage and evolution of  
642 landslide run-out and turbidity currents down submarine canyons, over tens of kilometres (e.g. Paull et  
643 al., 2018). The addition of co-located hydrophones and geophones to such moored or seafloor arrays will  
644 enable calibration of seismic and acoustic signals as well as determining threshold limits for detection.

645

#### 646 **5.2.5. Site-specific effects**

647 We suggest that different deployment configurations should be trialed to investigate how signals attenuate  
648 in different settings, as well as investigating the effects of increasing distance and differing angles of  
649 incidence from source. The effects of seafloor morphology may attenuate the signal generated by  
650 submarine landslides and complicate its propagation pathway, which is particularly important for  
651 directional instruments such as hydrophones. While hydrophones have been shown to detect events on  
652 relatively open delta slopes (Hay et al., 2021), to what extent the topographic effects of deeply-incised  
653 submarine canyons may limit detection of events by similar sensors placed outside the canyon, along  
654 narrow fjords or other irregular seafloor terrain remains poorly constrained. It is also important to identify  
655 and differentiate landslide-related noise from ambient seismic and acoustic noise that arises from natural  
656 background processes and human activities in the ocean. In noisy marine environments, ambient noise  
657 may overprint or entirely obscure the records of submarine landslides; hence, an understanding of the  
658 levels, frequency and time windows of that background noise is important when designing monitoring  
659 strategies (Lior et al., 2021). Societal lockdowns in 2020 and 2021 associated with the COVID-19  
660 pandemic have been identified as periods of significantly reduced seismic noise both on land and at sea  
661 (Lecocq et al., 2020; Ryan et al., 2020), and may therefore provide a rare window of reduced background

662 noise to explore local to global datasets. If signals can be sufficiently calibrated and confidently attributed  
663 to submarine landslides, historical records can be re-analysed to extend landslide catalogues in many  
664 regions worldwide, adding significant value to already valuable legacy datasets and providing new  
665 avenues for research and informing hazard management strategies.

666

### 667 **5.2.6. Challenges in data transfer**

668 As passive geophysical systems require much less power than active sensors (e.g. such as ADCPs), they  
669 can improve the endurance of offshore monitoring, lengthening monitoring windows in time. Future  
670 challenges still lie in transmission of data from sites that are far from shore (i.e. in abyssal to hadal water  
671 depths), particularly if an end goal is to support early-warning systems. This issue is largely moot for  
672 cabled systems as they support high bandwidth data transfer; although as already noted, the current reach  
673 of Distributed Acoustic Sensing limits long distance (>100s km) monitoring. For ocean bottom  
674 seismometers or hydrophones on seabed frames or moorings, there is currently no simple solution, as data  
675 file sizes typically exceed that currently permissible by acoustic data transmission.

676

### 677 **5.3. Suggestions for future directions**

678 We now finish by making some specific suggestions with regards to the future activities, listed in a  
679 broadly prioritised order.

680

#### 681 **5.3.1. Focus on calibration of hydrophone and geophone records at specific, well-known, 682 active sites**

683 We suggest that efforts should be focused on specific sites and settings to provide the calibration needed  
684 to strengthen confidence in the characterisation of submarine landslides from passive monitoring data. It  
685 is sensible to target active sites where previous monitoring has demonstrated regular landslide activity,  
686 where pre- and post-event bathymetric data are available, and where passive instruments (hydrophones,  
687 geophones, fibre-optic cables etc.) can be deployed concurrently with active sensors that record key  
688 parameters such as event timing, subsurface pore pressure, elevation changes, and flow velocity and  
689 sediment concentration. The Fraser Delta is one such location, being connected by seafloor cables to

690 Ocean Networks Canada's VENUS network (that enable real-time data transfer to shore) in an area of  
691 high sediment supply with sub-annual landslide activity. Synchronous deployment of hydrophones and  
692 seismometers, with current meters, inclinometers and piezometers (among other sensors) provides an  
693 ideal test bed for calibrated interpretation of seismic and acoustic signals attributed to small-scale  
694 submarine landslides (Lintern and Hill, 2010; Lintern et al, 2020). Other cable-connected sites, such as  
695 the EMSO (European Multidisciplinary Seafloor and water column Observatory) Ligure-Nice  
696 observatory provide opportunities to monitor the development of potential precursor conditions, but  
697 landslide recurrence is orders of magnitude lower at this site compared to the Fraser Delta; hence, the  
698 likelihood of catching a landslide itself is much less likely (Bompais et al., 2019). Similarly, the DONET  
699 (Dense Oceanfloor Network system for Earthquakes and Tsunamis) cabled sensor network located  
700 offshore SW Japan provides opportunities to detect submarine landslides, but intriguingly no evidence for  
701 such activity was found within a few hours of two large ( $>6 M_w$ ) earthquakes, with a study concluding  
702 that slopes may not be particularly susceptible to slope failure in that region (Gomberg et al., 2021).  
703 Indeed, most cabled observatories tend to avoid areas of very frequent landslide activity, so it will also be  
704 necessary to perform field calibration in other settings using more conventional landers or moorings that  
705 are not connected by cables, which requires sea-going research cruises. Sites with high, and predictable,  
706 sediment supply and where active field campaigns are planned will be the preferred candidates for  
707 synchronous deployment of active and passive monitoring equipment, such as major submarine canyons  
708 that connect to large rivers, or whose head intersects seasonally-variable littoral transport cells (e.g.  
709 canyons where sub-annual turbidity currents have previously been recorded: Congo Canyon, West Africa;  
710 Gaoping Canyon, Taiwan; Var Canyon, Mediterranean; Capbreton Canyon, Bay of Biscay; Khripounoff  
711 et al. 2012; Azpiroz-Zabala et al., 2017; Paull et al., 2018; Zhang et al., 2018). On a larger-scale, it will  
712 also be important to acquire data at active volcanic sites where onshore and offshore monitoring is on-  
713 going, such as the geodetic monitoring offshore Mount Etna, or land-based acoustic emission and GPS  
714 monitoring at Anak Krakatau (Urlaub et al., 2018; Walter et al., 2018). These activities should go hand in  
715 hand with efforts to determine site-specific effects on attenuation (e.g. due to topographic, substrate and  
716 other effects), which will benefit from numerical modelling to help identify and design the optimal sensor  
717 (e.g. where is the strongest or earliest signal expected?).

718

719       **5.3.2. Explore and calibrate existing land-based seismic monitoring data**

720 We suggest that more can, and should be, made of legacy broadband seismic datasets to explore past  
721 catalogues for evidence of submarine landslides. This method has been demonstrated offshore USA and  
722 Taiwan (Lin, 2015; Fan et al., 2020) and is more widely applicable, using data that have already been  
723 collected. Analysis of past time-series data should then be complemented with the acquisition of new  
724 seafloor survey data, to confirm that the spatial locations of landslide signals do indeed correspond with  
725 landslide events, and determine if a specific type(s) of landslide is more likely to generate a detectable  
726 seismic signal. This calibration will be most effective in areas where detailed swath multibeam echo-  
727 sounder surveys have already been performed (in particular high-resolution datasets acquired using  
728 Autonomous Underwater Vehicles), as differential elevations between multiple surveys provide a time  
729 window for a landslide, as well as its location. While repeat seafloor surveys are relatively rare, their use  
730 is growing, particularly in active submarine canyons (e.g. Smith et al., 2007; Paull et al., 2018), volcanic  
731 island flanks (e.g. Le Friant et al., 2010; Caplan-Auerbach et al., 2014; Hunt et al., 2021), offshore river  
732 deltas (e.g. Lintern et al., 2016; Obelcz et al., 2017), including across the Mississippi submarine delta  
733 where seafloor infrastructure is threatened by submarine slope failures (Chaytor et al., 2020; Obelcz et al.,  
734 2020). The footprint of these surveys tends to be quite limited; hence, it will most likely be necessary to  
735 target specific areas, focusing on acquiring high-resolution bathymetric data that enables identification of  
736 landslide scars and/or deposits. Evidence of landslide impacts on seafloor infrastructure (e.g. cable  
737 breaks, pipeline damage) may provide a useful addition point of calibration as this provides constraint on  
738 both timing and location of the event (e.g. Carter et al., 2014). Analysis of legacy seismic monitoring  
739 datasets, as well as new ones, will benefit from application of emergent machine learning techniques that  
740 permit analysis of vast datasets to train algorithms to automatically identify landslide events, and  
741 potentially identify previously-unrecognised environmental patterns that relate to landslide  
742 preconditioning (Thirugnanam et al., 2020; Deng et al., 2021).

743

744       **5.3.3. Calibrate and test fibre-optic detection of submarine landslides**

745 The emergence of fibre-optic sensing to monitor offshore geohazards (in particular Distributed Acoustic  
746 Sensing) is an exciting prospect, but one that currently remains unproven at field-scale for submarine  
747 landslide detection. The frequency ranges for detection appear to largely fall within the capabilities of  
748 Distributed Acoustic Sensing, although confident identification of low frequency ( $\ll 1$  Hz) signals may  
749 be challenging, particularly in noisy environments (e.g. due to natural ocean processes and human  
750 activities) or where cables are poorly coupled with the seafloor. Synchronous deployment of arrays of  
751 ocean bottom seismometers and hydrophones in active landslide settings are needed to provide the  
752 confidence in interpretation of Distributed Acoustic Sensing data as well as assessing the distance (both  
753 along-cable, and adjacent to it) over which measurements can reliably be made of the different signals  
754 created by submarine landslides. When installing new pipelines and cable, or when seafloor structures are  
755 decommissioned and left in situ, consideration could be given to integrate passive monitoring  
756 instrumentation to complement that used for monitoring infrastructure integrity (Wilcock et al., 2021). As  
757 SMART cables are installed (planned from 2024), opportunities will arise for accessing distributed sensor  
758 packages that may include hydrophones and/or geophones, adding valuable new potential locations for  
759 submarine landslide detection (Howe et al., 2019; Matias et al., 2021).

760

#### 761 **5.3.4. Extending the global monitoring network to enable operational early warning systems**

762 In the longer-term there is a need for expanded acoustic and seismic monitoring networks offshore; not  
763 only for detection of submarine landslides, but also for a host of ocean and earth science applications  
764 (Wilcock et al. 2021). Future opportunities may exist through collaboration with global monitoring  
765 programmes, such as MERMAIDS (Mobile Earthquake Recording in Marine Areas by Independent  
766 Divers), which employs a network of autonomous floats equipped with hydrophones (0.1-50 kHz) that  
767 passively drift across the ocean for deployments lasting up to five years; capable of transmitting  
768 seismograms in near real-time (Sukhovich et al., 2015; Hello and Nolet, 2020). Data gathered in such a  
769 manner may provide useful opportunistic snapshots of certain aspects of landslide activity, but may only  
770 yield limited data to answer outstanding science questions given the mobile nature of the floats and the  
771 lack of ground motion data. Therefore static seafloor sensors, rather than floating ones, will also be  
772 required, but a similar approach (i.e. that focuses developing low cost, and long endurance monitoring

773 platforms) is an important future direction. Whether seismic monitoring networks are extended offshore  
774 attached to cables, via distributed fibre-optic sensing, or using stand-alone moorings, seafloor landers or  
775 nodes, the development of more cost-effective sensors that do not require regular servicing, and are  
776 capable of transmitting data remotely, will transform our ability to monitor and ultimately provide early  
777 warning for submarine landslides. It is unlikely that we will fully rely upon passive monitoring  
778 approaches, but a future outlook could include automated decision-making by smart networks that  
779 determine whether a significant event has occurred, prompting the release of pop-up floats to transmit  
780 data, or active (high power-use) systems that are triggered to start recording, or switch to a higher  
781 sampling rate, by passive (lower power-use) sensors.

782

## 783 **6. Concluding remarks**

784 While there are still many open questions concerning submarine landslides and the hazards they pose, the  
785 recent growth in marine geophysical monitoring is rapidly providing data to start filling many of those  
786 gaps. Passive seismic and acoustic monitoring is in its relative infancy in this field, but has already shown  
787 significant promise in enabling the detection of submarine landslides over large areas, to ascertain their  
788 precise timing (and hence determine likely triggers), provide constraints on their transit velocity and run-  
789 out distance, and their effects (e.g. tsunami generation). We consider that these longer endurance and  
790 often more cost effective techniques are likely to form a complementary addition to existing approaches,  
791 rather than replace them entirely, particularly as many aspects of landslides can generate ground motions  
792 and/or acoustic noise. Ongoing calibration needs to be a priority to reliably discern and interpret signals  
793 generated by submarine landslides. Greater understanding through modeling will help to identify optimal  
794 sensor configurations. Distributed sensing along fibre-optic cables is an intriguing proposition, however,  
795 there is a compelling need to understand precisely what a submarine landslide signal looks like and over  
796 what spatial scale such signals can be reliably recorded. Studies are immediately required that test the  
797 sensitivity of passive landslide detection (using onshore and offshore networks) through concurrent  
798 deployment of active sensors. Once that calibration is performed across a breadth of sites and settings, we  
799 suggest that passive seismic and acoustic monitoring has the potential to answer a host of key,  
800 outstanding questions and significantly advance the field of submarine landslide science.

801

802 **7. Acknowledgements**

803 Clare and Talling acknowledge funding from the Natural Environment Research Council (NERC),  
804 including ‘Environmental Risks to Infrastructure: Identifying and Filling the Gaps’ (NE/ P005780/1),  
805 ‘New field-scale calibration of turbidity current impact modelling’ (NE/P009190/1), “Developing a  
806 Global Listening Network for Turbidity Currents and Seafloor Processes” (NE/S009965/1 and  
807 NE/S010068/1). The authors also acknowledge discussions with collaborators as part of Talling’s NERC  
808 International Opportunities Fund grant (NE/M017540/1) ‘Coordinating and pump-priming international  
809 efforts for direct monitoring of active turbidity currents at global test sites’. Clare also acknowledges  
810 support from the International Cable Protection Committee. Talling was supported by a NERC and Royal  
811 Society Industry Fellowship hosted by the International Cable Protection Committee. Additional funding  
812 for Clare was provided by NERC National Capability Climate Linked Atlantic Sector Science  
813 Programme (NE/R015953/1). E. Pope was supported by a Leverhulme Early Career Fellowship (ECF-  
814 2018-267). We thank Bruce Howe and an anonymous reviewer for constructive feedback that improved  
815 the manuscript.

816

817 **8. References**

- 818 Ai, F., Strasser, M., Preu, B., Hanebuth, T.J., Krastel, S. and Kopf, A., 2014. New constraints on  
819 oceanographic vs. seismic control on submarine landslide initiation: a geotechnical approach off  
820 Uruguay and northern Argentina. *Geo-Marine Letters*, 34(5), pp.399-417.
- 821 Ajo-Franklin, J.B., Dou, S., Lindsey, N.J., Monga, I., Tracy, C., Robertson, M., Tribaldos, V.R., Ulrich,  
822 C., Freifeld, B., Daley, T. and Li, X., 2019. Distributed acoustic sensing using dark fiber for near-  
823 surface characterization and broadband seismic event detection. *Scientific reports*, 9(1), pp.1-14.
- 824 Antsyferov, M.S., 1959. Seismo-Acoustic Methods in Mining (Consultants Bureau, New York, 1966);  
825 SD Vinogradov. *Bull. Acad. Sci. USSR Geophys. Ser.*, 2.
- 826 Azpiroz-Zabala, M., Cartigny, M.J., Talling, P.J., Parsons, D.R., Sumner, E.J., Clare, M.A., Simmons,  
827 S.M., Cooper, C. and Pope, E.L., 2017. Newly recognized turbidity current structure can explain  
828 prolonged flushing of submarine canyons. *Science advances*, 3(10), p.e1700200.

829 Batsi, E., Tsang-Hin-Sun, E., Klingelhoefer, F., Bayrakci, G., Chang, E.T., Lin, J.Y., Dellong, D.,  
830 Monteil, C. and Géli, L., 2019. Nonseismic Signals in the Ocean: Indicators of Deep Sea and Seafloor  
831 Processes on Ocean-Bottom Seismometer Data. *Geochemistry, Geophysics, Geosystems*, 20(8),  
832 pp.3882-3900.

833 Baumgartner, M.F., Stafford, K.M. and Latha, G., 2018. Near real-time underwater passive acoustic  
834 monitoring of natural and anthropogenic sounds. In *Observing the Oceans in Real Time* (pp. 203-226).  
835 Springer, Cham.

836 Besson, B., Eiríksson, G., Thórarinnsson, Ó., Thórarinnsson, A. and Einarsson, S., 2007. Automatic  
837 detection of avalanches and debris flows by seismic methods. *Journal of Glaciology*, 53(182), pp.461-  
838 472.

839 Biscara, L., Hanquiez, V., Leynaud, D., Marieu, V., Mulder, T., Gallissaires, J. M., Crespin, J.-P.,  
840 Braccini, E. and Garlan, T. (2012). Submarine slide initiation and evolution offshore Pointe Odden,  
841 Gabon-Analysis from annual bathymetric data (2004–2009). *Marine Geology*, 299, 43-50.

842 Blum, J.A., Chadwell, C.D., Driscoll, N. and Zumberge, M.A., 2010. Assessing slope stability in the  
843 Santa Barbara Basin, California, using seafloor geodesy and CHIRP seismic data. *Geophysical*  
844 *Research Letters*, 37(13).

845 Bompais, X., Garziglia, S., Blandin, J. and Hello, Y., 2019, June. EMSO-Ligure Nice, a Coastal Cabled  
846 Observatory Dedicated to the Study of Slope Stability. In *OCEANS 2019-Marseille* (pp. 1-8). IEEE.

847 Brackenridge, R.E., Nicholson, U., Sapiie, B., Stow, D. and Tappin, D.R., 2020. Indonesian Throughflow  
848 as a preconditioning mechanism for submarine landslides in the Makassar Strait. *Geological Society,*  
849 *London, Special Publications*, 500(1), pp.195-217.

850 Brodsky, E.E., Gordeev, E. and Kanamori, H., 2003. Landslide basal friction as measured by seismic  
851 waves. *Geophysical Research Letters*, 30(24).

852 Brothers, D.S., Luttrell, K.M. and Chaytor, J.D., 2013. Sea-level-induced seismicity and submarine landslide  
853 occurrence. *Geology*, 41(9), pp.979-982.

854 Brooks, H.L., Hodgson, D.M., Brunt, R.L., Peakall, J. and Flint, S.S., 2018. Exhumed lateral margins and  
855 increasing flow confinement of a submarine landslide complex. *Sedimentology*, 65(4), pp.1067-1096.

856 Bull, S., Arnot, M., Browne, G., Crundwell, M., Nicol, A. and Strachan, L., 2019. Neogene and  
857 Quaternary Mass-Transport Deposits From the Northern Taranaki Basin (North Island, New Zealand)  
858 Morphologies, Transportation Processes, and Depositional Controls. *Submarine Landslides:  
859 Subaqueous Mass Transport Deposits from Outcrops to Seismic Profiles*, pp.171-180.

860 Bull, S., Cartwright, J. and Huuse, M., 2009. A review of kinematic indicators from mass-transport  
861 complexes using 3D seismic data. *Marine and Petroleum Geology*, 26(7), pp.1132-1151.

862 Buss, C., Friedli, B. and Puzrin, A.M., 2019. Kinematic energy balance approach to submarine landslide  
863 evolution. *Canadian Geotechnical Journal*, 56(9), pp.1351-1365.

864 Cadman, J.D. and Goodman, R.E., 1967. Landslide noise. *Science*, 158(3805), pp.1182-1184.

865 Campbell, C.S., Cleary, P.W. and Hopkins, M., 1995. Large-scale landslide simulations: Global  
866 deformation, velocities and basal friction. *Journal of Geophysical Research: Solid Earth*, 100(B5),  
867 pp.8267-8283.

868 Campbell, K.J., Kinnear, S. and Thame, A., 2015. AUV technology for seabed characterization and  
869 geohazards assessment. *The leading edge*, 34(2), pp.170-178.

870 Caplan-Auerbach, J., Fox, C.G. and Duennebie, F.K., 2001. Hydroacoustic detection of submarine  
871 landslides on Kilauea volcano. *Geophysical Research Letters*, 28(9), pp.1811-1813

872 Caplan-Auerbach, J. and Huggel, C., 2007. Precursory seismicity associated with frequent, large ice  
873 avalanches on Iliamna volcano, Alaska, USA. *Journal of Glaciology*, 53(180), pp.128-140.

874 Caplan-Auerbach, J., Dziak, R.P., Bohnenstiehl, D.R., Chadwick, W.W. and Lau, T.K., 2014.  
875 Hydroacoustic investigation of submarine landslides at West Mata volcano, Lau Basin. *Geophysical  
876 Research Letters*, 41(16), pp.5927-5934.

877 Carter, L., Gavey, R., Talling, P.J. and Liu, J.T., 2014. Insights into submarine geohazards from breaks in  
878 subsea telecommunication cables. *Oceanography*, 27(2), pp.58-67.

879 Casas, D., Chiocci, F., Casalbore, D., Ercilla, G. and De Urbina, J.O., 2016. Magnitude-frequency  
880 distribution of submarine landslides in the Gioia Basin (southern Tyrrhenian Sea). *Geo-Marine  
881 Letters*, 36(6), pp.405-414.

882 Chadwick Jr, W.W., Dziak, R.P., Haxel, J.H., Embley, R.W. and Matsumoto, H., 2012. Submarine  
883 landslide triggered by volcanic eruption recorded by in situ hydrophone. *Geology*, 40(1), pp.51-54.

884 Chaytor, J.D., Baldwin, W.E., Bentley, S.J., Damour, M., Jones, D., Maloney, J., Miner, M.D., Obelcz, J.  
885 and Xu, K., 2020. Short-and long-term movement of mudflows of the Mississippi River Delta Front  
886 and their known and potential impacts on oil and gas infrastructure. *Geological Society, London,*  
887 *Special Publications*, 500(1), pp.587-604.

888 Chichibu, A., Jo, K., Nakamura, M., Goto, T. and Kamata, M., 1989. Acoustic emission characteristics of  
889 unstable slopes. *Journal of Acoustic Emission*, 8(4), pp.107-112.

890 Clare, M.A., Vardy, M.E., Cartigny, M.J., Talling, P.J., Himsforth, M.D., Dix, J.K., Harris, J.M.,  
891 Whitehouse, R.J. and Belal, M., 2017. Direct monitoring of active geohazards: Emerging geophysical  
892 tools for deep-water assessments. *Near Surface Geophysics*, 15(4), pp.427-444.

893 Clare, M., Lintern, D.G., Rosenberger, K., Clarke, J.E.H., Paull, C., Gwiazda, R., Cartigny, M.J., Talling,  
894 P.J., Perara, D., Xu, J. and Parsons, D., 2020. Lessons learned from the monitoring of turbidity  
895 currents and guidance for future platform designs. *Geological Society, London, Special*  
896 *Publications*, 500(1), pp.605-634.

897 Clare, M., Chaytor, J., Dabson, O., Gamboa, D., Georgiopolou, A., Eady, H., Hunt, J., Jackson, C., Katz,  
898 O., Krastel, S. and León, R., 2019. A consistent global approach for the morphometric characterization  
899 of subaqueous landslides. *Geological Society, London, Special Publications*, 477(1), pp.455-477.

900 Collico, S., Arroyo, M., Urgeles, R., Gràcia, E., Devincenzi, M. and Pérez, N., 2020. Probabilistic  
901 mapping of earthquake-induced submarine landslide susceptibility in the South-West Iberian  
902 margin. *Marine Geology*, 429, p.106296.

903 Cook, K.L., Andermann, C., Gimbert, F., Adhikari, B.R. and Hovius, N., 2018. Glacial lake outburst  
904 floods as drivers of fluvial erosion in the Himalaya. *Science*, 362(6410), pp.53-57

905 Cook, K.L., Rekapali, R., Dietze, M., et al. 2021. Detection and potential early warning of catastrophic  
906 flow events with regional seismic networks, *Science*, 374, 87-92.

907 Deng, L., Smith, A., Dixon, N. and Yuan, H., 2021. Machine learning prediction of landslide deformation  
908 behaviour using acoustic emission and rainfall measurements. *Engineering Geology*, p.106315.

909 Deparis, J., Jongmans, D., Cotton, F., Baillet, L., Thouvenot, F. and Hantz, D., 2008. Analysis of rock-  
910 fall and rock-fall avalanche seismograms in the French Alps. *Bulletin of the Seismological Society of*  
911 *America*, 98(4), pp.1781-1796.

912 Dewey, J. W., & Dellinger, J. A. (2008). Location of the Green Canyon (offshore southern Louisiana)  
913 seismic event of February 10, 2006, U.S. *Geological Survey Open-File Report*, **31p**, 2008– 1194.

914 Dixon, N. and Spriggs, M., 2007. Quantification of slope displacement rates using acoustic emission  
915 monitoring. *Canadian Geotechnical Journal*, *44*(8), pp.966-976.

916 Dixon, N., Spriggs, M.P., Smith, A., Meldrum, P. and Haslam, E., 2015. Quantification of reactivated  
917 landslide behaviour using acoustic emission monitoring. *Landslides*, *12*(3), pp.549-560.

918 Downs, P.W., Soar, P.J. and Taylor, A., 2016. The anatomy of effective discharge: the dynamics of  
919 coarse sediment transport revealed using continuous bedload monitoring in a gravel-bed river during a  
920 very wet year. *Earth Surface Processes and Landforms*, *41*(2), pp.147-161.

921 Dugan, B. (2012). Petrophysical and consolidation behavior of mass transport deposits from the northern  
922 Gulf of Mexico, IODP Expedition 308. *Marine Geology*, *315*, 98-107.

923 Ekström, G. and Stark, C.P., 2013. Simple scaling of catastrophic landslide  
924 dynamics. *Science*, *339*(6126), pp.1416-1419.

925 Fan, W., McGuire, J.J. and Shearer, P.M., 2020. Abundant spontaneous and dynamically triggered  
926 submarine landslides in the Gulf of Mexico. *Geophysical Research Letters*, *47*(12),  
927 p.e2020GL087213.

928 Frey-Martínez, J., Cartwright, J. and James, D., 2006. Frontally confined versus frontally emergent  
929 submarine landslides: A 3D seismic characterisation. *Marine and Petroleum Geology*, *23*(5), pp.585-  
930 604.

931 Fujiwara, T., dos Santos Ferreira, C., Bachmann, A.K., Strasser, M., Wefer, G., Sun, T., Kanamatsu, T.  
932 and Kodaira, S., 2017. Seafloor displacement after the 2011 Tohoku-Oki earthquake in the northern  
933 Japan trench examined by repeated bathymetric surveys. *Geophysical Research Letters*, *44*(23), pp.11-  
934 833.

935 Galitzin, B., 1915. Sur l'angle d'emergence des rayons sismiques. *Bull.(Izv.) Central Seismic Commission*  
936 *Russian Academy of Science*, *7*(2).

937 Gamboa, D., Omira, R. and Terrinha, P., 2021. A database of submarine landslides offshore West and  
938 Southwest Iberia. *Scientific Data*, *8*(1), pp.1-9.

939 Geay, T., Belleudy, P., Gervaise, C., Habersack, H., Aigner, J., Kreisler, A., Seitz, H. and Laronne, J.B.,  
940 2017. Passive acoustic monitoring of bed load discharge in a large gravel bed river. *Journal of*  
941 *Geophysical Research: Earth Surface*, 122(2), pp.528-545.

942 Geay, T., Zanker, S., Misset, C. and Recking, A., 2020. Passive Acoustic Measurement of Bedload  
943 Transport: Toward a Global Calibration Curve?. *Journal of Geophysical Research: Earth*  
944 *Surface*, 125(8), p.e2019JF005242.

945 Gee, M.J.R., Gawthorpe, R.L. and Friedmann, J.S., 2005. Giant striations at the base of a submarine  
946 landslide. *Marine Geology*, 214(1-3), pp.287-294.

947 Gee, M.J.R., Gawthorpe, R.L. and Friedmann, S.J., 2006. Triggering and evolution of a giant submarine  
948 landslide, offshore Angola, revealed by 3D seismic stratigraphy and geomorphology. *Journal of*  
949 *Sedimentary Research*, 76(1), pp.9-19.

950 Geist, E.L. and Parsons, T., 2010. Estimating the empirical probability of submarine landslide occurrence.  
951 In *Submarine mass movements and their consequences* (pp. 377-386). Springer, Dordrecht.

952 Goff, J. and Terry, J.P., 2016. Tsunamigenic slope failures: the Pacific Islands ‘blind  
953 spot’?. *Landslides*, 13(6), pp.1535-1543.

954 Gomberg, J., Ariyoshi, K., Hautala, S. and Johnson, H.P., The Finicky Nature of Earthquake Shaking-  
955 Triggered Submarine Sediment Slope Failures and Sediment Gravity Flows. *Journal of Geophysical*  
956 *Research: Solid Earth*, p.e2021JB022588.

957 Guiaستنec-Faugas, L., Gillet, H., Peakall, J., Dennielou, B., Gaillot, A. and Jacinto, R.S., 2021.  
958 Initiation and evolution of knickpoints and their role in cut-and-fill processes in active submarine  
959 channels. *Geology*, 49(3), pp.314-319.

960 Hampton, M.A., Lee, H.J. and Locat, J., 1996. Submarine landslides. *Reviews of geophysics*, 34(1),  
961 pp.33-59.

962 Harbitz, C.B., Løvholt, F. and Bungum, H., 2014. Submarine landslide tsunamis: how extreme and how  
963 likely?. *Natural Hazards*, 72(3), pp.1341-1374.

964 Hay, A.E., Hatcher, M.G. and Hughes Clarke, J.E., 2021. Underwater noise from submarine turbidity  
965 currents. *JASA Express Letters*, 1(7), p.0

966 Heerema, C.J., Talling, P.J., Cartigny, M.J., Paull, C.K., Bailey, L., Simmons, S.M., Parsons, D.R., Clare,  
967 M.A., Gwiazda, R., Lundsten, E. and Anderson, K., 2020. What determines the downstream evolution  
968 of turbidity currents?. *Earth and Planetary Science Letters*, 532, p.116023.

969 Heijnen, M.S., Clare, M.A., Cartigny, M.J., Talling, P.J., Hage, S., Lintern, D.G., Stacey, C., Parsons,  
970 D.R., Simmons, S.M., Chen, Y. and Sumner, E.J., 2020. Rapidly-migrating and internally-generated  
971 knickpoints can control submarine channel evolution. *Nature communications*, 11(1), pp.1-15.

972 Hello, Y. and Nolet, G., 2020. Floating seismographs (MERMAIDS). *Encyclopedia of Solid Earth*  
973 *Geophysics*, pp.1-6.

974 Hibert, C., Michéa, D., Provost, F., Malet, J.P. and Geertsema, M., 2019. Exploration of continuous  
975 seismic recordings with a machine learning approach to document 20 yr of landslide activity in  
976 Alaska. *Geophysical Journal International*, 219(2), pp.1138-1147.

977 Hizzett, J.L., Hughes Clarke, J.E., Sumner, E.J., Cartigny, M.J.B., Talling, P.J. and Clare, M.A., 2018.  
978 Which triggers produce the most erosive, frequent, and longest runout turbidity currents on  
979 deltas?. *Geophysical Research Letters*, 45(2), pp.855-863.

980 Howe, B.M., Arbic, B.K., Aucan, J., Barnes, C.R., Bayliff, N., Becker, N., Butler, R., Doyle, L., Elipot,  
981 S., Johnson, G.C. and Landerer, F., 2019. SMART cables for observing the global ocean: science and  
982 implementation. *Frontiers in Marine Science*, 6, p.424.

983 Hughes Clarke, J.E, Brucker, S., Muggah, J., Church, I., Cartwright, D., Kuus, P., Hamilton, T., Pratomo,  
984 D. and Eisan, B., 2012. The Squamish ProDelta: monitoring active landslides and turbidity currents.  
985 In *Canadian Hydrographic Conference 2012, Proceedings* (p. 15).

986 Hunt, J.E., Tappin, D.R., Watt, S.F.L., Susilohadi, S., Novellino, A, Ebmeier, S.K, Cassidy, M., Engwell,  
987 S.L., Grilli, S.T., Hanif, M., Priyanto, W.S., Clare, M.A., Abdurrachman, M., Udrek, U. 2021. (In  
988 Press). Submarine landslide megablocks show half of Anak Krakatau island failed on December 22nd,  
989 2018, *Nature Communications*.

990 Iannucci, R., Lenti, L. and Martino, S., 2020. Seismic monitoring system for landslide hazard assessment  
991 and risk management at the drainage plant of the Peschiera Springs (Central Italy). *Engineering*  
992 *Geology*, 277, p.105787.

- 993 Ide, S., Araki, E. and Matsumoto, H., 2021. Very broadband strain-rate measurements along a submarine  
994 fiber-optic cable off Cape Muroto, Nankai subduction zone, Japan. *Earth, Planets and Space*, 73(1),  
995 pp.1-10.
- 996 Inman, D.L., Nordstrom, C.E. and Flick, R.E., 1976. Currents in submarine canyons: An air-sea-land  
997 interaction. *Annual Review of Fluid Mechanics*, 8(1), pp.275-310.
- 998 Jeffreys, H., 1923. The Pamir Earthquake of 1911 February 18, in Relation to the Depths of Earthquake  
999 Foci. *Geophysical Journal International*, 1, pp.22-31.
- 1000 Kanamori, H. and Given, J.W., 1982. Analysis of long-period seismic waves excited by the May 18,  
1001 1980, eruption of Mount St. Helens—A terrestrial monopole?. *Journal of Geophysical Research: Solid  
1002 Earth*, 87(B7), pp.5422-5432.
- 1003 Kawakatsu, H., 1989. Centroid single force inversion of seismic waves generated by landslides. *Journal  
1004 of Geophysical Research: Solid Earth*, 94(B9), pp.12363-12374.
- 1005 Kelner, M., Migeon, S., Tric, E., Couboulex, F., Dano, A., Lebourg, T., & Taboada, A. (2016). Frequency  
1006 and triggering of small-scale submarine landslides on decadal timescales: Analysis of 4D bathymetric  
1007 data from the continental slope offshore Nice (France). *Marine Geology*, 379, 281-297.
- 1008 Khripounoff, A., Vangriesheim, A., Babonneau, N., Crassous, P., Dennielou, B. and Savoye, B., 2003.  
1009 Direct observation of intense turbidity current activity in the Zaire submarine valley at 4000 m water  
1010 depth. *Marine Geology*, 194(3-4), pp.151-158.
- 1011 Khripounoff, A., Crassous, P., Bue, N.L., Dennielou, B. and Jacinto, R.S., 2012. Different types of  
1012 sediment gravity flows detected in the Var submarine canyon (northwestern Mediterranean  
1013 Sea). *Progress in Oceanography*, 106, pp.138-153.
- 1014 Kioka, A., Schwesternmann, T., Moernaut, J., Ikehara, K., Kanamatsu, T., McHugh, C.M., dos Santos  
1015 Ferreira, C., Wiemer, G., Haghpor, N., Kopf, A.J. and Eglinton, T.I., 2019. Megathrust earthquake  
1016 drives drastic organic carbon supply to the hadal trench. *Scientific reports*, 9(1), pp.1-10
- 1017 Lacroix, P., Grasso, J.R., Roulle, J., Giraud, G., Goetz, D., Morin, S. and Helmstetter, A., 2012.  
1018 Monitoring of snow avalanches using a seismic array: Location, speed estimation, and relationships to  
1019 meteorological variables. *Journal of Geophysical Research: Earth Surface*, 117(F1).

- 1020 Lecocq, T., Hicks, S.P., Van Noten, K., Van Wijk, K., Koelemeijer, P., De Plaen, R.S., Massin, F.,  
1021 Hillers, G., Anthony, R.E., Apoloner, M.T. and Arroyo-Solórzano, M., 2020. Global quieting of high-  
1022 frequency seismic noise due to COVID-19 pandemic lockdown measures. *Science*, 369(6509),  
1023 pp.1338-1343.
- 1024 Leung, A.K. and Ng, C.W.W., 2016. Field investigation of deformation characteristics and stress  
1025 mobilisation of a soil slope. *Landslides*, 13(2), pp.229-240.
- 1026 Lin, C.H., 2015. Insight into landslide kinematics from a broadband seismic network. *Earth, planets and*  
1027 *space*, 67(1), p.8.
- 1028 Lin, C.H., Kumagai, H., Ando, M. and Shin, T.C., 2010. Detection of landslides and submarine slumps  
1029 using broadband seismic networks. *Geophysical Research Letters*, 37(22).
- 1030 Lindsey, N.J. and Martin, E.R., 2021. Fiber-Optic Seismology. Annual Review of Earth and Planetary  
1031 Sciences, 49, pp.309-336.+
- 1032 Lindsey, N.J., Dawe, T.C. and Ajo-Franklin, J.B., 2019. Illuminating seafloor faults and ocean dynamics  
1033 with dark fiber distributed acoustic sensing. *Science*, 366(6469), pp.1103-1107.
- 1034  
1035 Lintern, D. G., & Hill, P. R. (2010). An underwater laboratory at the Fraser River delta. *Eos, Transactions*  
1036 *American Geophysical Union*, 91(38), 333-334.
- 1037 Lintern, D. G., Hill, P. R., & Stacey, C. (2016). Powerful unconfined turbidity current captured by cabled  
1038 observatory on the Fraser River delta slope, British Columbia, Canada. *Sedimentology*.
- 1039 Lintern, D.G., Mosher, D.C. and Scherwath, M., 2019. Advancing from subaqueous mass movement case  
1040 studies to providing advice and mitigation. Geological Society, London, Special Publications, 477, 1-  
1041 14, 21 June 2019, <https://doi.org/10.1144/SP477-2018-190>
- 1042 Lior, I., Sladen, A., Rivet, D., Ampuero, J.P., Hello, Y., Becerril, C., Martins, H.F., Lamare, P., Jestin, C.,  
1043 Tsagkli, S. and Markou, C., 2021. On the Detection Capabilities of Underwater Distributed Acoustic  
1044 Sensing. *Journal of Geophysical Research: Solid Earth*, 126(3), p.e2020JB020925.
- 1045 Løvholt, F., Pedersen, G., Harbitz, C.B., Glimsdal, S. and Kim, J., 2015. On the characteristics of  
1046 landslide tsunamis. *Philosophical Transactions of the Royal Society A: Mathematical, Physical and*  
1047 *Engineering Sciences*, 373(2053), p.20140376.

- 1048 Mainsant, G., Larose, E., Brönnimann, C., Jongmans, D., Michoud, C. and Jaboyedoff, M., 2012.  
1049 Ambient seismic noise monitoring of a clay landslide: Toward failure prediction. *Journal of*  
1050 *Geophysical Research: Earth Surface*, 117(F1).
- 1051 Marra, G., Clivati, C., Lockett, R., Tampellini, A., Kronjäger, J., Wright, L., Mura, A., Levi, F.,  
1052 Robinson, S., Xuereb, A. and Baptie, B., 2018. Ultrastable laser interferometry for earthquake  
1053 detection with terrestrial and submarine cables. *Science*, 361(6401), pp.486-490.
- 1054 Maslin, M., Owen, M., Day, S. and Long, D., 2004. Linking continental-slope failures and climate  
1055 change: Testing the clathrate gun hypothesis. *Geology*, 32(1), pp.53-56.
- 1056 Masson, D.G., Harbitz, C.B., Wynn, R.B., Pedersen, G. and Løvholt, F., 2006. Submarine landslides:  
1057 processes, triggers and hazard prediction. *Philosophical Transactions of the Royal Society A:*  
1058 *Mathematical, Physical and Engineering Sciences*, 364(1845), pp.2009-2039.
- 1059 Mastbergen, D., van den Ham, G., Cartigny, M., Koelewijn, A., de Kleine, M., Clare, M., ... & Vellinga,  
1060 A. (2016). Multiple flow slide experiment in the Westerschelde Estuary, The Netherlands. In  
1061 *Submarine Mass Movements and their Consequences* (pp. 241-249). Springer International  
1062 Publishing.
- 1063 Matias, L.M., Carrilho, F., Sá, V., Omira, R., Niehus, M., Corela, C., Barros, J. and Omar, Y., 2021. The  
1064 contribution of submarine optical fiber telecom cables to the monitoring of earthquakes and tsunamis  
1065 in the NE Atlantic. *Frontiers in Earth Science*, 9, p.611.
- 1066 McAdoo, B.G., Pratson, L.F. and Orange, D.L., 2000. Submarine landslide geomorphology, US  
1067 continental slope. *Marine Geology*, 169(1-2), pp.103-136.
- 1068 Mecozzi, A., Cantono, M., Castellanos, J.C., Kamalov, V., Muller, R. and Zhan, Z., 2021. Polarization  
1069 sensing using submarine optical cables. *Optica*, 8(6), pp.788-795.
- 1070 Michlmayr, G., Chalari, A., Clarke, A. and Or, D., 2017. Fiber-optic high-resolution acoustic emission  
1071 (AE) monitoring of slope failure. *Landslides*, 14(3), pp.1139-1146.
- 1072 Miramontes, E., Garziglia, S., Sultan, N., Jouet, G. and Cattaneo, A., 2018. Morphological control of  
1073 slope instability in contourites: a geotechnical approach. *Landslides*, 15(6), pp.1085-1095.

1074 Mizutani, A., Yomogida, K. and Tanioka, Y., 2020. Early tsunami detection with near-fault ocean-bottom  
1075 pressure gauge records based on the comparison with seismic data. *Journal of Geophysical Research:*  
1076 *Oceans*, 125(9), p.e2020JC016275.

1077 Moernaut, J. and De Batist, M., 2011. Frontal emplacement and mobility of sublacustrine landslides:  
1078 results from morphometric and seismostratigraphic analysis. *Marine Geology*, 285(1-4), pp.29-45.

1079 Mohrig, D. and Marr, J.G., 2003. Constraining the efficiency of turbidity current generation from  
1080 submarine debris flows and slides using laboratory experiments. *Marine and Petroleum*  
1081 *Geology*, 20(6-8), pp.883-899.

1082

1083 Moore, J.G., Clague, D.A., Holcomb, R.T., Lipman, P.W., Normark, W.R. and Torresan, M.E., 1989.  
1084 Prodigious submarine landslides on the Hawaiian Ridge. *Journal of Geophysical Research: Solid*  
1085 *Earth*, 94(B12), pp.17465-17484.

1086 Moretti, L., Allstadt, K., Mangeney, A., Capdeville, Y., Stutzmann, E. and Bouchut, F., 2015. Numerical  
1087 modeling of the Mount Meager landslide constrained by its force history derived from seismic  
1088 data. *Journal of Geophysical Research: Solid Earth*, 120(4), pp.2579-2599.

1089 Mountjoy, J.J., McKean, J., Barnes, P.M. and Pettinga, J.R., 2009. Terrestrial-style slow-moving  
1090 earthflow kinematics in a submarine landslide complex. *Marine geology*, 267(3-4), pp.114-127.

1091 Mountjoy, J.J., Howarth, J.D., Orpin, A.R., Barnes, P.M., Bowden, D.A., Rowden, A.A., Schimel, A.C.,  
1092 Holden, C., Horgan, H.J., Nodder, S.D. and Patton, J.R., 2018. Earthquakes drive large-scale  
1093 submarine canyon development and sediment supply to deep-ocean basins. *Science advances*, 4(3),  
1094 p.eaar3748.

1095 Mulder, T. and Cochonat, P., 1996. Classification of offshore mass movements. *Journal of Sedimentary*  
1096 *research*, 66(1), pp.43-57.

1097 Nisbet, E.G. and Piper, D.J., 1998. Giant submarine landslides. *Nature*, 392(6674), pp.329-330.

1098 Nishimura, T., Emoto, K., Nakahara, H., Miura, S., Yamamoto, M., Sugimura, S., Ishikawa, A. and  
1099 Kimura, T., 2021. Source location of volcanic earthquakes and subsurface characterization using fiber-  
1100 optic cable and distributed acoustic sensing system. *Scientific reports*, 11(1), pp.1-12.

- 1101 Normandeau, A., Campbell, D.C., Piper, D.J. and Jenner, K.A., 2019. Are submarine landslides an  
1102 underestimated hazard on the western North Atlantic passive margin?. *Geology*, 47(9), pp.848-852.
- 1103 Normandeau, A., MacKillop, K., Macquarrie, M., Richards, C., Bourgault, D., Campbell, D.C., Maselli,  
1104 V., Philibert, G. and Clarke, J.H., 2021. Submarine landslides triggered by iceberg collision with the  
1105 seafloor. *Nature Geoscience*, 14(8), pp.599-605.
- 1106 Nwoko, J., Kane, I. and Huuse, M., 2020. Megaclasts within mass-transport deposits: their origin,  
1107 characteristics and effect on substrates and succeeding flows. *Geological Society, London, Special  
1108 Publications*, 500(1), pp.515-530.
- 1109 Obelcz, J., Xu, K., Georgiou, I.Y., Maloney, J., Bentley, S.J. and Miner, M.D., 2017. Sub-decadal  
1110 submarine landslides are important drivers of deltaic sediment flux: Insights from the Mississippi  
1111 River Delta Front. *Geology*, 45(8), pp.703-706.
- 1112 Obelcz, J., Wood, W.T., Phrampus, B.J. and Lee, T.R., 2020. Machine learning augmented time-lapse  
1113 bathymetric surveys: A case study from the Mississippi river delta front. *Geophysical Research  
1114 Letters*, 47(10), p.e2020GL087857.
- 1115 Ogata, K., Festa, A. and Pini, G.A. eds., 2019. *Submarine Landslides: Subaqueous Mass Transport  
1116 Deposits from Outcrops to Seismic Profiles* (Vol. 247). John Wiley & Sons.
- 1117 Parker, G., 1982. Conditions for the ignition of catastrophically erosive turbidity currents. *Marine  
1118 Geology*, 46(3-4), pp.307-327.
- 1119 Paull, C.K., Talling, P.J., Maier, K.L., Parsons, D., Xu, J., Caress, D.W., Gwiazda, R., Lundsten, E.M.,  
1120 Anderson, K., Barry, J.P. and Chaffey, M., 2018. Powerful turbidity currents driven by dense basal  
1121 layers. *Nature communications*, 9(1), pp.1-9.
- 1122 Paull, C.K., Ussler, W. and Holbrook, W.S., 2007. Assessing methane release from the colossal Storegga  
1123 submarine landslide. *Geophysical research letters*, 34(4).
- 1124 Piper, D.J., Cochonat, P. and Morrison, M.L., 1999. The sequence of events around the epicentre of the  
1125 1929 Grand Banks earthquake: initiation of debris flows and turbidity current inferred from sidescan  
1126 sonar. *Sedimentology*, 46(1), pp.79-97.
- 1127 Pope, E.L., Talling, P.J., Carter, L., Clare, M.A. and Hunt, J.E., 2017. Damaging sediment density flows  
1128 triggered by tropical cyclones. *Earth and Planetary Science Letters*, 458, pp.161-169.

- 1129 Puzrin, A.M., Germanovich, L.N. and Friedli, B., 2016. Shear band propagation analysis of submarine  
1130 slope stability. *Géotechnique*, 66(3), pp.188-201.
- 1131 Prior, D.B., Bornhold, B.D., Coleman, J.M. and Bryant, W.R., 1982. Morphology of a submarine slide,  
1132 Kitimat arm, British Columbia. *Geology*, 10(11), pp.588-592.
- 1133 Prior, D.B., Suhayda, J.N., Lu, N.Z., Bornhold, B.D., Keller, G.H., Wiseman, W.J., Wright, L.D. and  
1134 Yang, Z.S., 1989. Storm wave reactivation of a submarine landslide. *Nature*, 341(6237), pp.47-50
- 1135 Puzrin, A.M., Germanovich, L.N. and Friedli, B., 2016. Shear band propagation analysis of submarine  
1136 slope stability. *Géotechnique*, 66(3), pp.188-201.
- 1137 Ranasinghe, N., Rowe, C., Syracuse, E., Larmat, C. and Begnaud, M., 2018. Enhanced global seismic  
1138 resolution using transoceanic SMART cables. *Seismological Research Letters*, 89(1), pp.77-85.
- 1139 Rickenmann, D., 2017. Bedload transport measurements with geophones, hydrophones and underwater  
1140 microphones (passive acoustic methods). *Gravel Bed Rivers and Disasters*, Wiley & Sons, Chichester,  
1141 UK, pp.185-208.
- 1142 Roche, B., Bull, J.M., Marin-Moreno, H., Leighton, T.G., Falcon-Suarez, I.H., Tholen, M., White, P.R.,  
1143 Provenzano, G., Lichtschlag, A., Li, J. and Faggetter, M., 2021. Time-lapse imaging of CO2 migration  
1144 within near-surface sediments during a controlled sub-seabed release experiment. *International  
1145 Journal of Greenhouse Gas Control*, 109, p.103363.
- 1146 Rouse, C., Styles, P. and Wilson, S.A., 1991. Microseismic emissions from flowslide-type movements in  
1147 South Wales. *Engineering Geology*, 31(1), pp.91-110.
- 1148 Ryan, J.P., Joseph, J.E., Margolina, T., Peavey Reeves, L., Hatch, L., DeVogelaere, A., Southall, B.,  
1149 Stimpert, A. and Baumann-Pickering, S., 2020. Quieting of low-frequency vessel noise in Monterey  
1150 Bay National Marine Sanctuary during the COVID-19 pandemic. *The Journal of the Acoustical  
1151 Society of America*, 148(4), pp.2734-2734.
- 1152 Sammartini, M., Moernaut, J., Kopf, A., Stegmann, S., Fabbri, S.C., Anselmetti, F.S. and Strasser, M.,  
1153 2021. Propagation of frontally confined subaqueous landslides: Insights from combining geophysical,  
1154 sedimentological, and geotechnical analysis. *Sedimentary Geology*, p.105877.

- 1155 Sgroi, T., Monna, S., Embriaco, D., Giovanetti, G., Marinaro, G. and Favali, P., 2014. Geohazards in the  
1156 western Ionian Sea: Insights from non-earthquake signals recorded by the NEMO-SN1 seafloor  
1157 observatory. *Oceanography*, 27(2), pp.154-166.
- 1158 Simmons, S.M., Azpiroz-Zabala, M., Cartigny, M.J.B., Clare, M.A., Cooper, C., Parsons, D.R., Pope,  
1159 E.L., Sumner, E.J. and Talling, P.J., 2020. Novel acoustic method provides first detailed  
1160 measurements of sediment concentration structure within submarine turbidity currents. *Journal of*  
1161 *Geophysical Research: Oceans*, 125(5), p.e2019JC015904.
- 1162 Smith, D.P., Kvitek, R., Iampietro, P.J. and Wong, K., 2007. Twenty-nine months of geomorphic change  
1163 in upper Monterey Canyon (2002–2005). *Marine Geology*, 236(1-2), pp.79-94.
- 1164 Stegmann, S., Sultan, N., Kopf, A., Apprioual, R., & Pelleau, P. (2011). Hydrogeology and its effect on  
1165 slope stability along the coastal aquifer of Nice, France. *Marine Geology*, 280(1), 168-181.
- 1166 Strasser, M., Kölling, M., Ferreira, C.D.S., Fink, H.G., Fujiwara, T., Henkel, S., Ikehara, K., Kanamatsu,  
1167 T., Kawamura, K., Kodaira, S. and Römer, M., 2013. A slump in the trench: Tracking the impact of  
1168 the 2011 Tohoku-Oki earthquake. *Geology*, 41(8), pp.935-938.
- 1169 Strout, J. M., & Tjelta, T. I. (2005). In situ pore pressures: What is their significance and how can they be  
1170 reliably measured?. *Marine and Petroleum Geology*, 22(1), 275-285.
- 1171 Sukhovich, A., Bonnieux, S., Hello, Y., Irissou, J.O., Simons, F.J. and Nolet, G., 2015. Seismic  
1172 monitoring in the oceans by autonomous floats. *Nature communications*, 6(1), pp.1-6.
- 1173 Sultan, N., Savoye, B., Jouet, G., Leynaud, D., Cochonat, P., Henry, P., Stegmann, S. and Kopf, A., 2010.  
1174 Investigation of a possible submarine landslide at the Var delta front (Nice continental slope, southeast  
1175 France). *Canadian Geotechnical Journal*, 47(4), pp.486-496.
- 1176 Sumner, E.J. and Paull, C.K., 2014. Swept away by a turbidity current in Mendocino submarine canyon,  
1177 California. *Geophysical Research Letters*, 41(21), pp.7611-7618.
- 1178 Suriñach, E., Vilajosana, I., Khazaradze, G., Biescas, B., Furdada, G. and Vilaplana, J.M., 2005. Seismic  
1179 detection and characterization of landslides and other mass movements. *Natural Hazards and Earth*  
1180 *System Sciences*, 5(6), pp.791-798.

1181 Talling, P.J., Paull, C.K. and Piper, D.J., 2013. How are subaqueous sediment density flows triggered,  
1182 what is their internal structure and how does it evolve? Direct observations from monitoring of active  
1183 flows. *Earth-Science Reviews*, 125, pp.244-287.

1184 Talling, P.J., Wynn, R.B., Masson, D.G., Frenz, M., Cronin, B.T., Schiebel, R., Akhmetzhanov, A.M.,  
1185 Dallmeier-Tiessen, S., Benetti, S., Weaver, P.P.E. and Georgiopoulou, A., 2007. Onset of submarine  
1186 debris flow deposition far from original giant landslide. *Nature*, 450(7169), pp.541-544.

1187 Tappin, D.R., Grilli, S.T., Harris, J.C., Geller, R.J., Masterlark, T., Kirby, J.T., Shi, F., Ma, G.,  
1188 Thingbaijam, K.K.S. and Mai, P.M., 2014. Did a submarine landslide contribute to the 2011 Tohoku  
1189 tsunami?. *Marine Geology*, 357, pp.344-361.

1190 Tappin, D.R., Watts, P. and Grilli, S.T., 2008. The Papua New Guinea tsunami of 17 July 1998: anatomy  
1191 of a catastrophic event. *Natural Hazards and Earth System Sciences*, 8(2), pp.243-266.

1192 Ten Brink, U.S., Geist, E.L. and Andrews, B.D., 2006. Size distribution of submarine landslides and its  
1193 implication to tsunami hazard in Puerto Rico. *Geophysical Research Letters*, 33(11).

1194 Ten Brink, U., Twichell, D., Geist, E., Chaytor, J., Locat, J., Lee, H., Buczkowski, B., Barkan, R., Solow,  
1195 A., & Andrews, B. (2008). Evaluation of tsunami sources with the potential to impact the US Atlantic  
1196 and Gulf coasts, U.S. Geological Survey Administrative report to the US Nuclear Regulatory  
1197 Commission 300.

1198 Thirugnanam, H., Ramesh, M.V. and Rangan, V.P., 2020. Enhancing the reliability of landslide early  
1199 warning systems by machine learning. *Landslides*, 17(9), pp.2231-2246.

1200 Urgeles, R. and Camerlenghi, A., 2013. Submarine landslides of the Mediterranean Sea: Trigger  
1201 mechanisms, dynamics, and frequency-magnitude distribution. *Journal of Geophysical Research:*  
1202 *Earth Surface*, 118(4), pp.2600-2618.

1203 Urlaub, M., Petersen, F., Gross, F., Bonforte, A., Puglisi, G., Guglielmino, F., Krastel, S., Lange, D. and  
1204 Kopp, H., 2018. Gravitational collapse of Mount Etna's southeastern flank. *Science Advances*, 4(10),  
1205 p.eaat9700.

1206 Urlaub, M., Talling, P.J. and Masson, D.G., 2013. Timing and frequency of large submarine landslides:  
1207 implications for understanding triggers and future geohazard. *Quaternary Science Reviews*, 72, pp.63-  
1208 82.

1209 Urlaub, M., Talling, P.J. and Clare, M., 2014. Sea-level-induced seismicity and submarine landslide  
1210 occurrence: Comment. *Geology*, 42(6), pp.e337-e337.

1211 Urlaub, M. and Villinger, H., 2019. Combining in situ monitoring using seabed instruments and  
1212 numerical modelling to assess the transient stability of underwater slopes. *Geological Society, London,*  
1213 *Special Publications*, 477(1), pp.511-521.

1214 Vanneste, M., Sultan, N., Garziglia, S., Forsberg, C. F., & L'Heureux, J. S. (2014). Seafloor instabilities  
1215 and sediment deformation processes: the need for integrated, multi-disciplinary investigations. *Marine*  
1216 *Geology*, 352, 183-214.

1217 Van Herwijnen, A., Heck, M. and Schweizer, J., 2016. Forecasting snow avalanches using avalanche  
1218 activity data obtained through seismic monitoring. *Cold Regions Science and Technology*, 132, pp.68-  
1219 80.

1220 Van Herwijnen, A. and Schweizer, J., 2011. Seismic sensor array for monitoring an avalanche start zone:  
1221 design, deployment and preliminary results. *Journal of Glaciology*, 57(202), pp.267-276.

1222 Vardy, M.E., L'Heureux, J.S., Vanneste, M., Longva, O., Steiner, A., Forsberg, C.F., Haflidason, H. and  
1223 Brendryen, J., 2012. Multidisciplinary investigation of a shallow near-shore landslide, Finneidfjord,  
1224 Norway. *Near Surface Geophysics*, 10(4), pp.267-277.

1225 Waage, M., Singhroha, S., Bünz, S., Planke, S., Waghorn, K.A. and Bellwald, B., 2021. Feasibility of  
1226 using the P-Cable high-resolution 3D seismic system in detecting and monitoring CO2  
1227 leakage. *International Journal of Greenhouse Gas Control*, 106, p.103240.

1228 Walter, T.R., Haghighi, M.H., Schneider, F.M., Coppola, D., Motagh, M., Saul, J., Babeyko, A., Dahm,  
1229 T., Troll, V.R., Tilmann, F. and Heimann, S., 2019. Complex hazard cascade culminating in the Anak  
1230 Krakatau sector collapse. *Nature communications*, 10(1), pp.1-11.

1231 Wilcock, W., 2021. Illuminating tremors in the deep. *Science*, 371(6532), pp.882-884.

1232 Williams, E.F., Fernández-Ruiz, M.R., Magalhaes, R., Vanthillo, R., Zhan, Z., González-Herráez, M. and  
1233 Martins, H.F., 2019. Distributed sensing of microseisms and teleseisms with submarine dark  
1234 fibers. *Nature communications*, 10(1), pp.1-11.

1235 Xu, J.P., 2010. Normalized velocity profiles of field-measured turbidity currents. *Geology*, 38(6), pp.563-  
1236 566.

1237 Xu, J.P., 2011. Measuring currents in submarine canyons: Technological and scientific progress in the  
1238 past 30 years. *Geosphere*, 7(4), pp.868-876.

1239 Yamada, M., Kumagai, H., Matsushi, Y. and Matsuzawa, T., 2013. Dynamic landslide processes revealed  
1240 by broadband seismic records. *Geophysical Research Letters*, 40(12), pp.2998-3002.

1241 Ye, L., Kanamori, H., Rivera, L., Lay, T., Zhou, Y., Sianipar, D. and Satake, K., 2020. The 22 December  
1242 2018 tsunami from flank collapse of Anak Krakatau volcano during eruption. *Science advances*, 6(3),  
1243 p.eaaz1377.

1244 Yeh, Y.C., Tsai, C.L., Hsu, S.K., Lin, H.S., Chen, K.T., Cho, Y.Y. and Liang, C.W., 2021. Continental  
1245 shelf morphology controlled by bottom currents, mud diapirism, and submarine slumping to the east  
1246 of the Gaoping Canyon, off SW Taiwan. *Geo-Marine Letters*, 41(1), pp.1-11.

1247 Yuan, X., Kind, R. and Pedersen, H.A., 2005. Seismic monitoring of the Indian Ocean  
1248 tsunami. *Geophysical research letters*, 32(15).

1249 Zeng, J., Lowe, D.R., Prior, D.B., Wiseman JR, W.J. and Bornhold, B.D., 1991. Flow properties of  
1250 turbidity currents in Bute Inlet, British Columbia. *Sedimentology*, 38(6), pp.975-996.

1251 Zhan, Z., 2020. Distributed acoustic sensing turns fiber-optic cables into sensitive seismic  
1252 antennas. *Seismological Research Letters*, 91(1), pp.1-15.

1253 Zhan, Z., Cantono, M., Kamalov, V., Mecozzi, A., Müller, R., Yin, S. and Castellanos, J.C., 2021.  
1254 Optical polarization-based seismic and water wave sensing on transoceanic  
1255 cables. *Science*, 371(6532), pp.931-936.

1256 Zhang, Y., Liu, Z., Zhao, Y., Colin, C., Zhang, X., Wang, M., Zhao, S. and Kneller, B., 2018. Long-term  
1257 in situ observations on typhoon-triggered turbidity currents in the deep sea. *Geology*, 46(8), pp.675-  
1258 678.

1259 Zhao, S., Wang, Z., Nie, Z., He, K. and Ding, N., 2021. Investigation on total adjustment of the  
1260 transducer and seafloor transponder for GNSS/Acoustic precise underwater point positioning. *Ocean  
1261 Engineering*, 221, p.108533.

1262